Spring 2019

Interactions of Gold Thiolates with Protein Disulfides

Anna Tyrina

INTERACTIONS OF GOLD THIOLATES WITH PROTEIN DISULFIDES

By

Anna Tyrina

A Thesis Submitted in Partial Fulfillment

Of the Requirements for a Degree with Honors

(Chemistry)

The Honors College

University of Maine

May 2019

Advisory Committee:

Dr. Alice Bruce, Chair and Professor of Chemistry Department, Advisor

Dr. Mitchell Bruce, Professor of Chemistry

Dr. Carl Tripp, Professor of Chemistry

Dr. Francois Amar, Dean of the Honors College

Dr. Melissa Ladenheim, Associate Dean of the Honors College

ABSTRACT

This thesis research focuses on the interaction of gold(I) thiolates with the disulfide bonds in proteins, using insulin as a model protein. Insulin contains three disulfide bonds that can break apart during thiol-disulfide exchange reactions. The goal of this research was to compare the reactivity of aromatic thiols and gold(I) thiolates in thiol-disulfide exchange reactions with insulin. When the disulfide bonds in insulin are cleaved, a suspension of the beta chain particles forms, which scatters 650 nm light, therefore making it convenient to monitor the reaction using UV-Vis spectroscopy. The rate of formation of the colloidal suspension is taken to be directly proportional to the rate of disulfide bond breakage, as reported by Lees, et al.[1] who studied the ability of aromatic thiols to catalyze the reaction of dithiothreitol (DTT) and insulin. The project began by measuring the relative rate of the reaction between 4-mercaptobenzoic acid, DTT and insulin vs DTT and insulin, which was also done by the Lees research group. All reactions were conducted at room temperature in pH 6.5 phosphate buffered solution. The rate of disulfide bind cleavage in the reaction of 4-mercaptobenzoic acid, DTT and insulin was 1.7 times faster than the reaction of DTT and insulin. This is consistent with the relative rate of 1.6 reported by Lees, et al.[1] and provided confidence that using the light scattering technique described by Lees, et al. to monitor the reactions with insulin was a viable method in our lab. Another experiment was conducted to see whether 4-mercaptobenzoic acid would react with insulin by itself; however, this reaction did not produce a colloidal suspension within a 24-hour period of time, which suggests that 4-mercaptobenzoic acid does not cleave the disulfide bonds in insulin in the absence of DTT. The reaction between 2-mercaptopyridine (Spy), DTT and insulin was also

investigated, and it was determined that 2-mercaptopyridine behaves similarly to 4-mercaptobenzoic acid. The next set of experiments was conducted to determine the effect of replacing aromatic thiols with gold(I) thiolates. Addition of $Et_3PAu(Spy)$ to a solution of DTT and insulin caused cleavage of the disulfide bonds in insulin, as observed by an increase of light scattering at 650 nm. The shape of the absorbance (intensity of light scattering) vs. time graph suggests two or more possible competing mechanisms. This is further supported by the observation that $Et_3PAu(Spy)$ reacts with DTT and insulin separately. In the reaction of $Et_3PAuSpy$ and insulin, there is formation of a colloidal suspension while in the reaction between $Et_3PAuSpy$ and DTT, 2-mercaptopyridine is produced, as evidenced by UV-Vis and ^1H NMR spectroscopy. The findings of the study suggest that $Et_3PAu(Spy)$ undergoes a thiol disulfide exchange reaction with insulin, causing precipitation of the β-chains. Furthermore, this reaction occurs in the absence of DTT, which is different than the reactivity of aromatic thiols. It is not known whether the Et_3PAu moiety binds to one of the insulin chains or whether further reaction occurs. Additional studies should be done to deduce the mechanism of the reaction. Et_3PAuCl was also shown to react with insulin, resulting in the formation of a precipitate. Since Et_3PAuCl cannot undergo thiol disulfide exchange, it is suggested that Et_3PAuCl interacts with other donor atoms such as histidine residues in insulin, instead of interacting with the disulfide bonds, but further studies should be done to deduce the mechanism of the reaction.

ACKNOWLEDGEMENTS

I would like to start by thanking Dr. Alice Bruce for her endless encouragement, advice, willingness to troubleshoot experiments and always being excited about new things I unearthed from the literature. It has been a privilege to work in a supporting scientific environment. I would also like to thank my thesis committee (Dr. Alice Bruce, Dr. Mitchell Bruce, Dr. Francois Amar, Dr. Melissa Ladenheim and Dr. Carl Tripp) for being willing to listen and encourage me when I came in last minute to ask for help or just told them about the progress I have made. I would like to thank Dr. Matthew Brichacek for showing me the Chimera program, one of the most useful tools for anyone working with proteins. I would also like to thank Dr. Carl Tripp for making me absolutely love working in Excel. I would like to thank S. Max Bessey for teaching me how to maneuver through the jungle that is our UV-Vis software and for his Excel template that allowed for easier data processing, when I was dealing with hundreds of spectra. Our research group also deserves a lot of credit for helping me find glassware, clean NMR tubes, uncontaminated reagents and teaching me the various skills one can only learn by observation and experience. I would like to thank the Charlie Slavin Grant for the financial support in the purchase of chemicals. I would also like to thank Dr. Brian Frederick for his continued support and his constant effort to make me a better person and scientist. I would like to thank all of my friends in the Chemistry Department who have enriched my experience at UMaine and saved me more times than I can count. Lastly, I would like to thank my parents, Valentina Tyrina and Lou Niles, for their continual and unwavering support and love.

TABLE OF CONTENTS

INTRODUCTION

Insulin contains three disulfide bonds that can break apart during thiol-disulfide exchange reactions, forming a suspension of the beta chain particles, which scatters 650 nm light, therefore making it convenient to monitor the reaction using UV-Vis spectroscopy, where the rate of formation of the colloidal suspension is taken to be directly proportional to the rate of disulfide bond breakage. Aromatic thiols have been shown to increase the rate of disulfide bond breakage in the reaction between dithiothreitol (DTT) and insulin, where DTT and the aromatic thiol can act as redox buffers. A redox buffer is composed of a redox couple; in this case a reducing thiol and corresponding oxidized disulfide. A redox buffer is analogous to an acid-base buffer in that a species that is in abundance in solution will be neutralized by the corresponding component of the redox couple[2]. The same way that the conjugate acid in a buffer neutralizes an added base, thiol reduces an added oxidant and disulfide oxidizes a reduced species. A redox buffer is an aide in protein folding. In terms of physiology, the ratio of thiol to disulfide is an important factor in helping to maintain redox homeostasis for healthy functioning of the organism. For example, glutathione (GSH) is the most abundant antioxidant in aerobic cells, present in micromolar concentrations in bodily fluids and millimolar concentrations in tissue[3]. GSH is critical for protecting the brain from oxidative stress, with a normal percent of GSH compared to the corresponding disulfide (GSSG) of 98%[3]. This ratio of GSH/GSSG is reduced in neurodegenerative diseases, such as Parkinson's disease and Alzheimer's disease[3]. The abundant research that has been conducted on glutathione ratios in humans shows that the ratio is an important factor in the development of disease. Thus, it is important to study redox buffers as potential ways of understanding the mechanisms of

these diseases. The following study was conducted to observe the effect of gold thiolates on biological disulfides, using insulin as a model protein disulfide. It was predicted that gold thiolates might act as a redox buffer, much in the same way that an aromatic thiol would in the reaction between DTT and insulin.

Goals of Research

The major question of this study is concerned with how gold thiolates may be interacting with biological disulfide proteins such as insulin. The hypothesis entails the use of gold thiolate as a redox buffer, much in the same way that an aromatic thiol/thiolate can act as a redox buffer in the reaction between insulin and DTT (where DTT also acts as a redox buffer). The Lees research group has done extensive research on the aspects of a protein folding redox buffer that would be most advantageous for the rate and yield of protein folding, and has specified the following criteria for advantages to the redox buffer:

1) Low thiol pKa (strongly acidic thiol, weakly basic thiolate-close to physiological pH), a pKa of approximately 1 unit less than the pH of the solution has been found to be optimal for protein folding, because of the enhanced reactivity of the thiolate[4]
2) Low reduction potential (allows the redox buffer to exist as a nearly 50:50 mixture of thiol and disulfide for efficient protein folding)[4]
3) Dithiol over a monothiol (dithiols discourage forming long-lived mixed disulfides between the folding catalyst and the protein of interest)
4) Aromatic over aliphatic increases the rate of folding by at least three times

The Lees research group had published a paper in 2012 on the synthesis and protein folding rates of aromatic dithiols, combining the two advantages (dithiol and aromatic) to make a power duo[5], but they have not attempted to do the same for metals, such as gold. Before such attempts are made it is important to see if a gold thiolate would react with a protein disulfide and if so, if it would act as a redox buffer. The plan is to conduct a set of UV-Vis and ^{1}H NMR experiments to investigate the reactions of gold complexes, thiols and insulin to observe possible interactions between the reactants that would hint at the possibility of gold thiolate acting as a redox buffer. Starting with the reaction between insulin, DTT and an aromatic thiol, the goal is to replace the aromatic thiol with a gold thiolate and observe the interaction. Along the way, several other experiments will be conducted, such as the reaction between DTT and a gold thiolate, to look at possible side reactions.

Gold in Medicine

Gold has been used medicinally to treat various diseases for many centuries. The use of gold dates as far back as 2500 BC, the earliest application of gold as a therapeutic in China[6,7]. The modern interest in gold is attributed to the discovery by Robert Koch in 1890 that gold cyanide inhibits the growth of *Tubercle bacillus*, the bacterium that causes tuberculosis in humans[6,7]. Despite the lack of experimental evidence and the toxicity of the compound, the "gold decade" followed (1925-1935), in which intravenously administered gold(I) thiolate salts were used for the treatment of tuberculosis[6,7]. During this time, gold therapy was also found to reduce joint pain in a group of non-tubercular patients, which led Jacques Forestier, a French physician, to research the use of gold

compounds as a treatment for rheumatoid arthritis[6,7]. Subsequently, in 1960 a trial concluded that gold drugs have a beneficial effect for the treatment of rheumatoid arthritis[6,7]. Some gold thiolate drugs that were first introduced in the 1920's are still used today (Figure 1). These drugs primarily slow the progression of disease. Auranofin (Figure 1.3) is an orally active drug. Despite early indications that auranofin offered significant advantages over injectable Au(I) thiolates, it was later proven that auranofin is, in fact, less effective[6,7]. Because of this, oral gold is now rarely used clinically[6,7].

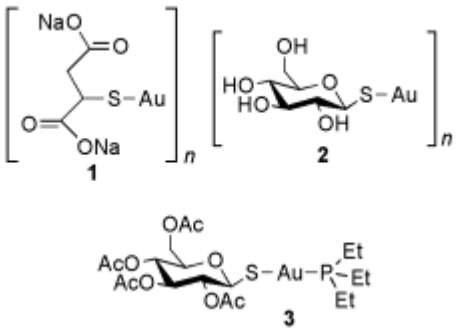

Figure 1: Examples of gold(I) drugs used for the treatment of rheumatoid arthritis (**1**) sodium aurothiomalate (Myocrisin), (**2**) aurothioglucose (Solganol), (**3**) tetraacetyl-B-d-thioglucose gold(I) triethylphosphine (auranofin). The 1:1 Au-S drugs (**1** and **2**) are polymers[6].

Gold Thiolates as Treatment for Rheumatoid Arthritis

Specifically, gold thiolates are used to treat rheumatoid arthritis, which is a chronic inflammatory disease characterized by the migration of activated phagocytes and leukocytes into synovial tissue, which causes progressive destruction of cartilage and bone and joint swelling[6,7]. There is evidence that gold thiolates have several different ways they help treat the disease, where most cases involve interaction with protein Cys (or Sec) residues[6,7]. Recent studies on gold thiolate mechanisms have focused on their effects on macrophage signal transduction and the induction of inflammatory cytokines[6,7]. Cytokines are low molecular weight peptides, proteins or glycoproteins[6,7].

Gold compounds can play a role in each of the phases of the immune reaction, such as the initiation stage[6,7]. During this stage, gold is taken up by macrophages and inhibits antigen processing[6,7]. This likely happens by binding peptide antigens that contain cysteine and methionine residues[6,7]. Gold then accumulates, in the form of S-Au(I)-S, in the lysosomes of synovial cells and macrophages, forming aurosomes (gold laden deposits)[6,7]. At the level of transcription, gold(I) drugs downregulate a range of proinflammatory genes by inhibiting transcriptional activities of the NF-kB and AP-1 (Jun/Fos) transcription factors[7]. In general, AP-1 controls the expression of genes for collagenase and the cytokine IL-2, and NF-kB controls transcription of other inflammatory mediators, including TNF-α, IL-1, and IL-6[7]. Additionally, gold drugs act at the T-cell level, and have been shown to inhibit osteoclast bone resorption, recently attributed to the inhibition of the cathepsins[6,7]. Rheumatoid arthritis patients also have elevated levels of copper that can be correlated to the severity of the disease[6,7]. This might be because gold drugs could interfere with copper homeostasis by binding Cu(I) responsive transcription factors and other Cu(I) transport proteins[6,7].

Gold drugs are classified as DMARDS (disease-modifying anti-rheumatic drugs). Despite the fact that DMARDS are one of the only ways to place the inflammatory disease in remission, they are slow acting, sometimes requiring 3-6 months for patients to experience improvement in joint function and reduction in swelling[8].

Other Medicinal Uses of Gold

In addition to being used as rheumatoid arthritis medications, Au(I) and Au(III) compounds have also been used and designed with an aim of targeting cellular components that are implicated at the onset or progression of cancers, as well as viral and

parasitic diseases[6,7]. In the mid 1980's auranofin (Figure 1.3) was shown to inhibit the growth of cultured tumor cells[6]. Since then, a large variety of Au(I) and Au(III) complexes has been developed that show some kind of inhibition of tumor growth and have been shown to have potential as cancer treatments[6]. In addition, various Au(I) antitumor compounds, including auranofin, have been shown to overcome resistance to cisplatin and other anticancer drugs[7]. Many mechanistic studies indicate mitochondria as the biological targets for gold antitumor compounds since mitochondria play a key role in the regulation of apoptosis and the regulation of the intracellular redox state[7].

Gold-based compounds also showed early promise as a less toxic and less drug resistant version of an AIDS cure[6]. A variety of Au(I) and Au(III) compounds have been investigated as anti-HIV agents[6]. Gold-based compounds also offer great potential in the field of affordable antiparasitic drugs[6]. This is because they can bind thiol and selenol proteins that have been identified as drug targets in trypanosomes (African sleeping sickness, Chagas' disease and leishmaniasis), malaria-causing plasmodia, and schistomiasis[6]. In conclusion, there is great potential for application of the gold complex mechanisms for treatment of a variety of diseases, and for the design of new gold complexes for diseases with the same target complexes.

Gold Compounds

Gold(I) ($5d^{10}$) is a large ion with a low charge and is a "soft" Lewis acid, therefore forming its most stable complexes with "soft" ligands such as CN, S-donors, P-donors and Se ligands[7]. Linear, two-coordination is most common for gold(I)[7]. The highest affinity gold(I) has is for thiols with the lowest pK_a values[7].

There are examples in the literature of gold(I) complexes facilitating disulfide bond cleavage in biologically relevant systems[9,10]. Early studies on auranofin (Figure 1.3) show that its highly reactive nature towards protein thiols limits its antitumor activity *in vivo*[6]. Subsequently, the development of Au(I) complexes with chelated diphosphines such as $[Au(dppe)_2]Cl$ (Figure 2) began with the goal of reducing the high thiol reactivity of auronofin and similar compounds. The behavior of this compound is consistent with that of the class of antitumor agents known as delocalized lipophilic cations (DLCs), that accumulate in the mitochondria of tumor cells driven by one of the characteristic features of some cancer cells- an elevated mitochondrial membrane potential[6]. It was found that the high lipophilicity of these compounds results in severe toxicity as a consequence of the inability of the compounds to differentiate between tumorigenic and non-tumorigenic cells, concentrating in both and causing general membrane permeabilization[6]. A compound was designed to retain the lipophilic cationic properties of the tetrahedral bis-chelated complexes that allow accumulation into the mitochondria, but reduce the cytotoxicity of the compound, so it can be used as an anti-tumor agent[1]. This compound was $[Au(d2pypp)_2]Cl$, and recent findings have shown that the compound is selectively toxic to breast cancer cells but not normal breast cells.

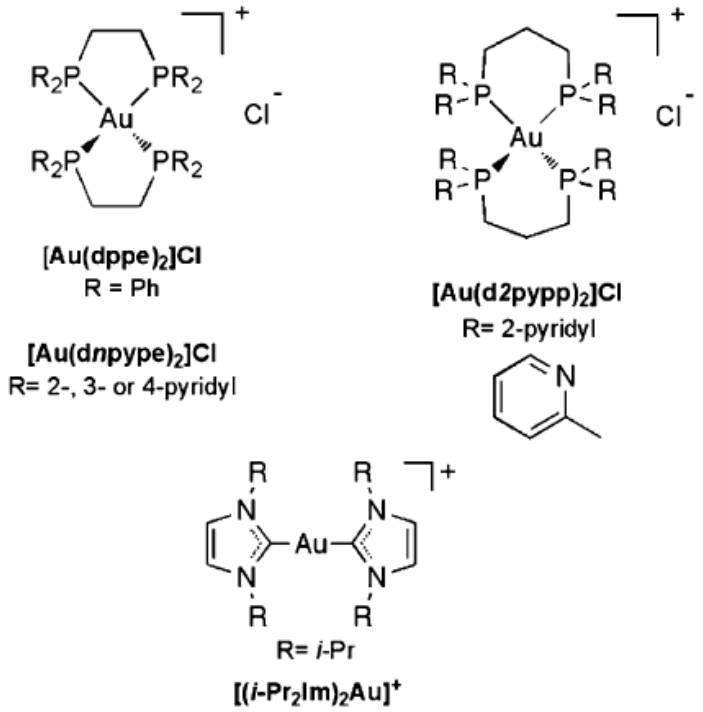

Figure 2: Examples of lipophilic cationic gold(I) antitumor compounds[6].

Similar compounds were used as the focus of this investigation. Specifically, Et_3PAuCl, $Et_3PAuSpy$ (where py is a 2-pyridyl group), and $Et_3PAuSba$ (where ba is a benzoic acid group) (Figure 3).

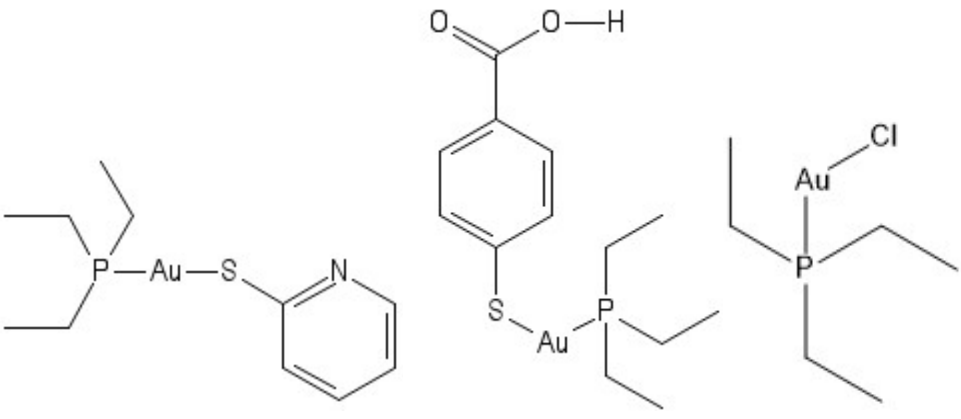

Figure 3: From left to right: structures of $Et_3PAuSpy$, $Et_3PAuSba$ and Et_3PAuCl respectively.

$Et_3PAuSpy$ has been shown to have antitumor effects *in vivo* (mice) and has also been shown to have a similar cytotoxicity to auranofin *in vitro* (P388 leukemia cells)[11]. Et_3PAuCl was less cytotoxic *in vitro* but had the same maximally tolerated dose in tumor bearing mice, on a daily x5 ip (intraperitoneal injection) regimen[11]. Between the two compounds, $Et_3PAuSpy$ had a larger antitumor effect (46% median life span (ILS) increase in mice inoculated ip with 10^6 P388 leukemia cells, given ip on days 1-5) versus Et_3PAuCl (36% ILS increase), where an ILS value of ≥40% represents cell kill sufficient to result in net reduction in tumor cell burden at the end of therapy; with a level of significance of $p \leq 0.05$[11]. Early mechanistic studies provided evidence that Et_3PAuCl affects mitochondrial function and these results are consistent with an antitumor mechanism involving the induction of mitochondrial-dependent apoptosis pathways[7].

It is of interest to note that some studies have hypothesized that the more reactive the gold compound is towards disulfide bonds, the more toxic it probably is[9]. This hypothesis stems from the observation that the more a compound is like auranofin structurally, the more easily it breaks disulfide bonds and the likelihood that the biological activity of the compound will be similar to auranofin increases, therefore making the compound supposedly more toxic.

Thiols

The thiols used in this study include dithiothreitol (DTT), 4-mercaptobenzoic acid (Sba), and 2-mercaptopyridine (Spy) (Figure 4).

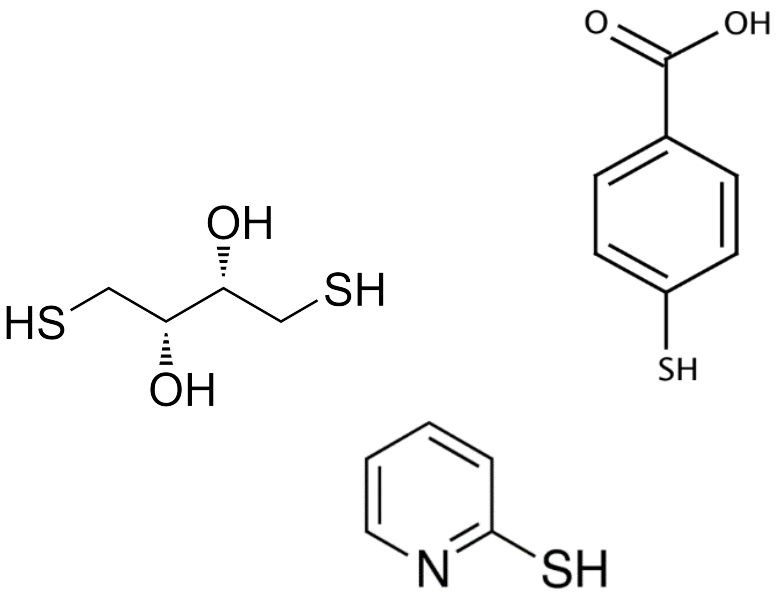

Figure 4: Thiols used in this study from left to right: dithiothreitol (DTT) (pKa=9.2, 10.1), 4-mercaptobenzoic acid (Sba) (pKa=5.95), and 2-mercaptopyridine.

It is known that 4-mercaptobenzoic acid increases the activity of protein disulfide isomerase (PDI) by a factor of three[12]. PDI is a eukaryotic enzyme that has many functions during the folding of disulfide-containing proteins (Figure 5)[12]. In terms of a mechanism, PDI functions in the same way as an aromatic thiol when in solution with a protein disulfide. It is also known that 4-mercaptobenzoic acid catalyzes the reaction between insulin and DTT[1]. PDI contains two active sites, each of which has a CXXC motif, where X is any amino acid and C is cysteine[4]. The two cysteines form a 14-membered ring upon oxidation to the disulfide[4].

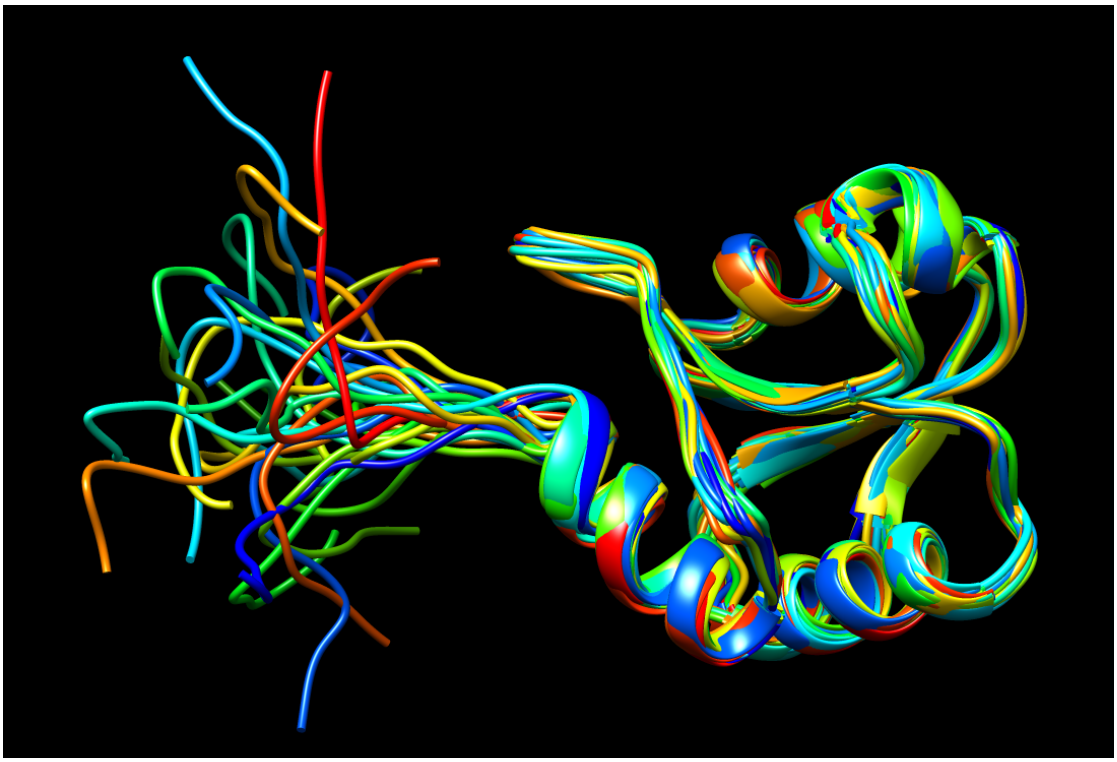

Figure 5: Structure of protein disulfide isomerase (PDI). Backbones are indicated as rounded ribbons, which are part of α-helices or β-sheets. The string-like filaments are parts of loops and turns (different kind of protein organisation). Each color is a different chain. The chains come together to form PDI. Picture constructed using Chimera viewing software (PDB file:2BJX, protein disulfide isomerase)

DTT itself can act as a buffer by having a mix of reduced thiol DTT and oxidized disulfide DTT, which forms a redox buffer, a mix of thiol (RSH) and corresponding disulfide (RSSR)[1,12]. Dithiols, like DTT, are proposed to improve protein folding by shortening the lifetime of kinetically stable mixed disulfide formed between the protein and the small molecule thiol[13]. Having two thiols makes it easier for DTT to displace the mixed disulfide intramolecularly instead of intermolecularly, as is the case for monothiols, where intramolecular displacement is proposed to be more rapid[13]. DTT has been studied extensively for its reducing capabilities when in contact with disulfides. As the reduced DTT is not UV-active, one can use the oxidized DTT formed in the process

of thiol-disulfide exchange to quantify the number of disulfide bonds broken by measuring the absorbance at 310 nm, where the molar absorption of DTT is 40% of its maximum absorbance[14]. The number of SH groups per mole protein was measured by rapid gel filtration with the method of Ellman (see source 10 citation 8). DTT has also been studied for its proposed activities in stimulating the insulin receptor/kinase, which is the initial event of insulin action (binding of insulin to its receptor on the cell surface of target cells[15]. Some studies focused on the calorimetric measurements of the reduction of insulin by DTT, which allows to approximate the number of protons attached to cysteine residues in insulin after reduction, thereby approximating the degree to which the disulfide bonds in insulin have been reduced[16,17].

An advantage that PDI has over monothiols is the availability of two thiols at each active site. There is a proposed advantage for dithiols that has been termed the "escape mechanism" that allows the dithiol to discourage the formation of long-lived mixed disulfides between the folding catalyst and the protein of interest (Figure 6)[4].

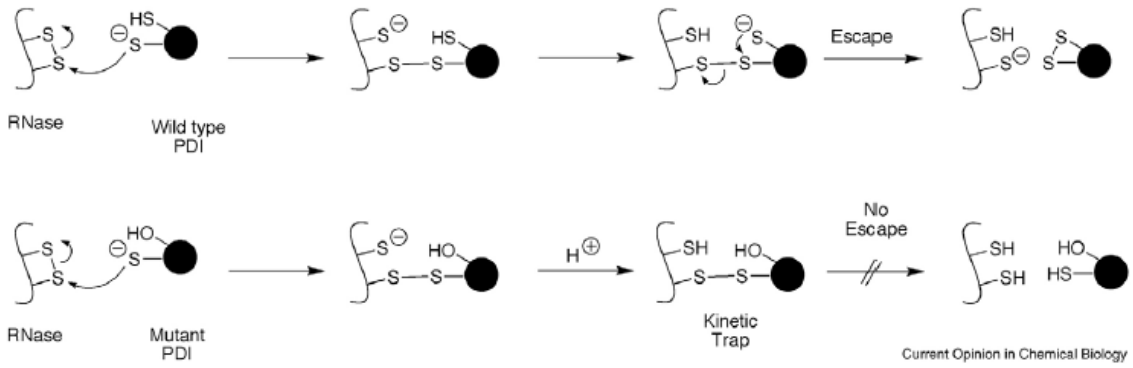

Figure 6: Proposed advantage of having two thiols in each active site of PDI, the escape mechanism[4]

In 2012 the Lees group published a paper detailing the synthesis of aromatic dithiols that were used as potential redox buffers for the folding of inclusion bodies (protein aggregates) into the native functional form of the protein disulfide[5]. The aromatic dithiols significantly increased the folding rate and also the yield of functional protein compared to aliphatic monothiols, aliphatic dithiols and even aromatic monothiols[5]. The Lees group has also recently proposed that aromatic thiols with an elongated alkyl group on the aromatic ring are expected to increase interactions with the hydrophobic core of disulfide containing proteins during folding, allowing easier access to buried disulfide bonds[18].

Insulin

Overview

Insulin is a hormone that plays an important role in the regulation of vertebrate metabolism[19]. It is also the most important pharmaceutical peptide for the treatment of diabetes[20]. This project uses insulin as a model protein disulfide because it contains three disulfide bonds that can break apart during thiol-disulfide exchange reactions, forming a suspension of α- and β-chain particles[1,21], which scatters 650 nm light[22] therefore making it convenient to monitor the reaction using UV-Vis spectroscopy. It has been shown that these unfolded chains expose their hydrophobic surfaces and bind together through hydrophobic interactions, eventually forming large, insoluble aggregates[20]. The wavelength of 650 nm was picked specifically because it shows a linear relationship between S-S bond reduction and precipitation[22]. Insulin contains 1 intra-chain disulfide bond on the α-chain (A6-A11) and 2 inter-chain disulfide bonds (A20-B19, A7-B7) that hold the α and the β chains together (Figure 7). It was found by Holmgren that the rate of precipitation of the insulin chains was much higher at pH 6.5 than at pH 8.0[22]. This is consistent with the fact that insulin is less soluble at lower pH.

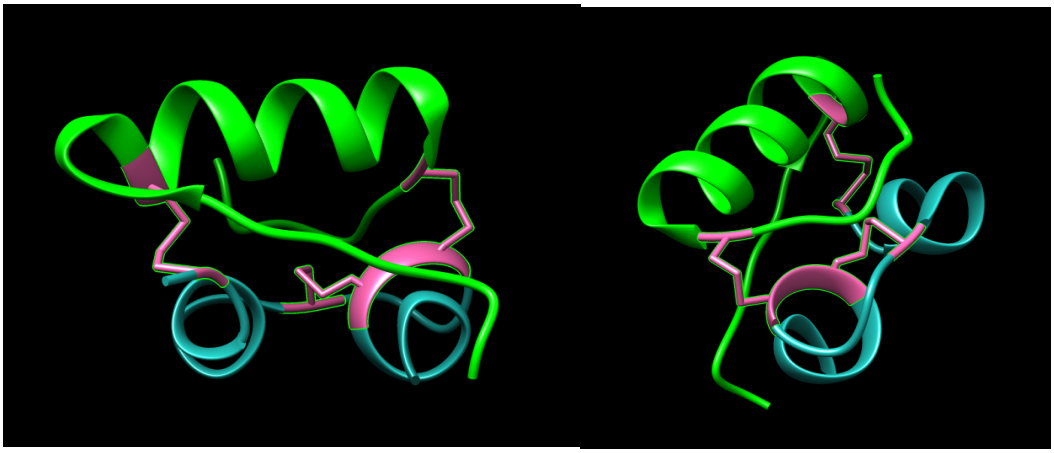

Figure 7: Structure of insulin, showing the α-chain (blue), β-chain (green) and the Cys-Cys disulfide bonds (pink). Picture constructed using Chimera viewing software (PDB file: 6QQ7, bovine insulin).

Typically, disulfide bonds are formed by the oxidation of cysteine residues and provide stability to the protein by minimizing the entropy of the unfolded state as they crosslink one part of the protein with another[4]. This oxidative protein folding mechanism mainly occurs inside the endoplasmic reticulum of eukaryotes[4]. All three disulfide bonds are essential for the receptor binding activity of insulin but contribute differently to the overall structure[23]. Deletion of the second interchain disulfide bond (A20-B19) has the most substantial influence on the structure as indicated by the loss of ordered secondary structure, increased susceptibility to proteolysis, and greatly reduced compactness[23]. This is most likely due to the fact that this bridge packs within itself a cluster of conserved aliphatic and aromatic side chains in the hydrophobic core[19]. The deletion of the intrachain disulfide bond causes the least change in the structure[23]. It is also known that the disulfide bonds are formed sequentially in the order A20-B19, A7-B7 and A6-A11 in the folding pathway of proinsulin (where A and B are the α and β chains and the number

designates placement of connecting amino acid in the amino acid sequence of insulin) (Figure 8).[19,23]

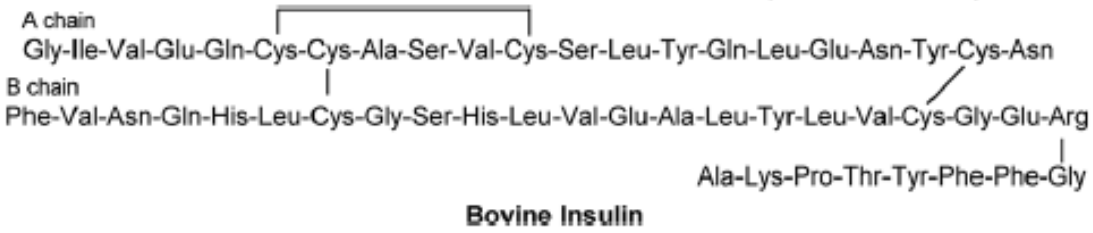

Figure 8: Bovine insulin amino acid sequence, with disulfide bonds indicated as a solid line[24]

These disulfide bonds are formed when proinsulin, the precursor to insulin, is folded in the endoplasmic reticulum prior to packaging into secretory granules in pancreatic β-cells which already contain the requisite processing enzymes[23,25]. The adult hormone is stored as Zn^{2+} stabilized hexamers (Figure 10) within these granules[19]. The hexamers precipitate in the granules, which increases the stability of mature insulin, making it inaccessible to proteases[26]. The hexamers dissociate upon secretion into the portal circulation, since only the monomeric form of insulin is able to bind its receptors in the liver and adipose tissue[19,26]. The zinc-mediated assembly may represent a defense against toxic misfolding in the secretory granule (Figure 9)[19].

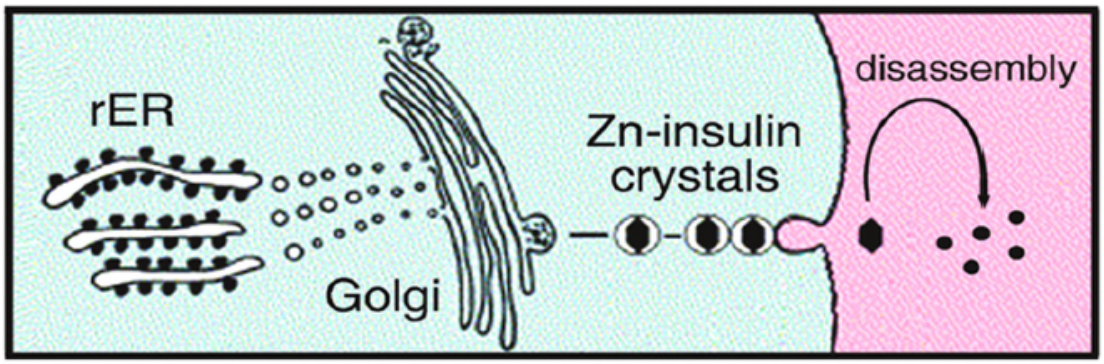

Figure 9: β-cell biosynthetic pathway for the packaging of insulin[19].

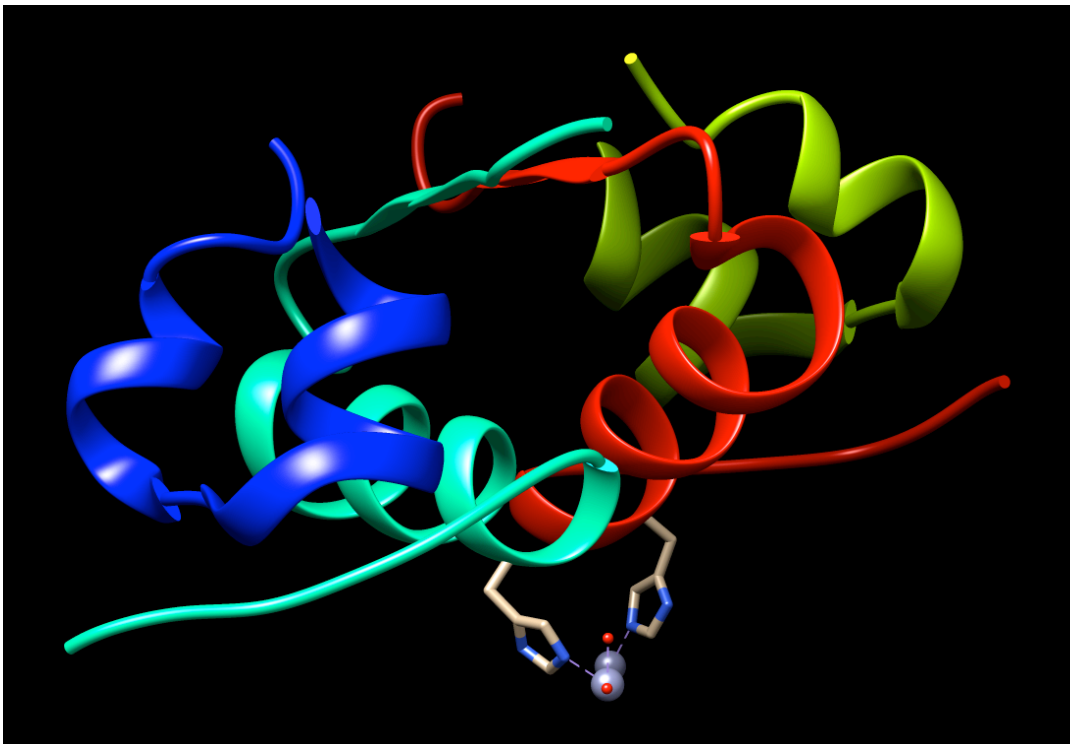

Figure 10: View of insulin dimer coordinated by histidine residues to 2 Zn^{2+} atoms (grey spheres). By combining with two other dimers, insulin forms a zinc-stabilized hexamer. The hexamer also contains a Ca^{2+} cation for increased stability. Picture constructed using Chimera viewing software (PDB file: 2ins).

The disulfide bonds that hold the two chains of insulin together are post translational modifications involved in stabilizing the native structure[27]. Research has shown that it is not only the interchain disulfide bonds that are broken in a reduction reaction of insulin,

but when treated with thioglycolate solutions at pH 5, the major reaction that occurs is the cleavage of the intrachain disulfide bond on the α-chain[21]. It is not clear which of the three total disulfide bonds in the structure are more accessible to reagents and is therefore the likely candidate to be reduced first, although some researchers suppose that the intrachain disulfide bond will be reduced first[21]. Other researchers have pointed out that the rate of *electrolytic* reduction of the two interchain bonds was found to be significantly faster than that of the intrachain disulfide bond[28]. It seems that the likelihood of being reduced first depends on the experimental conditions and reagents used.

In terms of accessibility, it seems like the A7-B7 inter disulfide bond is most accessible (exposed) based on a ball and stick model in Figure 11 (right). Additionally, because the hydrophobicity surface is pointed out (remember that B7 is surrounded by leucine and glycine, which are both hydrophobic) the molecule will want to expose the hydrophilic cysteine in the same way a micelle will want to fold the hydrophobic tails in a lipid bilayer inside itself while exposing the hydrophilic heads. On the other hand, the A20-B19 and A6-A11 disulfide bonds have hydrophobicity pockets, which might be big enough to fit a gold thiolate molecule inside but are not quite as accessible.

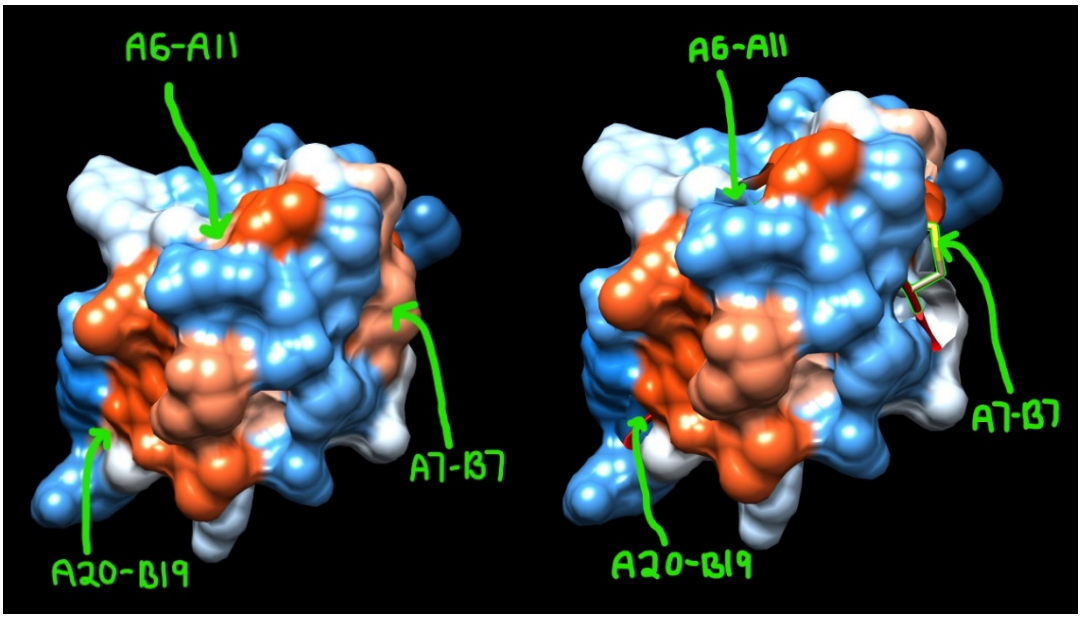

Figure 11: Hydrophobicity surface of insulin, where the color gradient is determined by the Kyte-Doolittle scale, where blue is hydrophilic, red is hydrophobic and white is in between. Picture at right shows the cysteine residue hydrophobicity surface removed. Picture constructed using Chimera viewing software (PDB file: 6QQ7, bovine insulin).

Each amino acid residue has an alpha carbon and two Ramachandran angles: ψ-psi and φ-phi, the only two bonds that are available to freely rotate in the backbone, and therefore define the conformation of the protein. ψ is the angle between C_α and the carbonyl carbon (Figures 12 and 13), while φ is the angle between C_α and the amide that joins two residues together (Figures 14 and 15). The Ramachandran plot can be seen in Figure 16. Ψ and φ are limited by steric hinderance, as no two atoms may occupy the same space, and these regions of the Ramachandran plot will therefore be empty of any residues. These regions are not allowed by sterics.

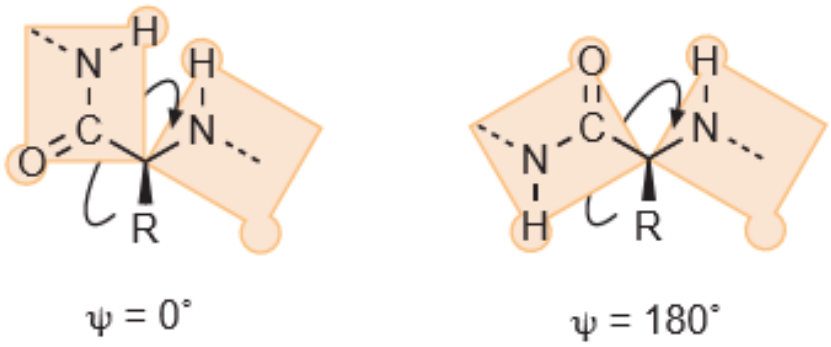

Figure 12: Rotation of psi bond[29]

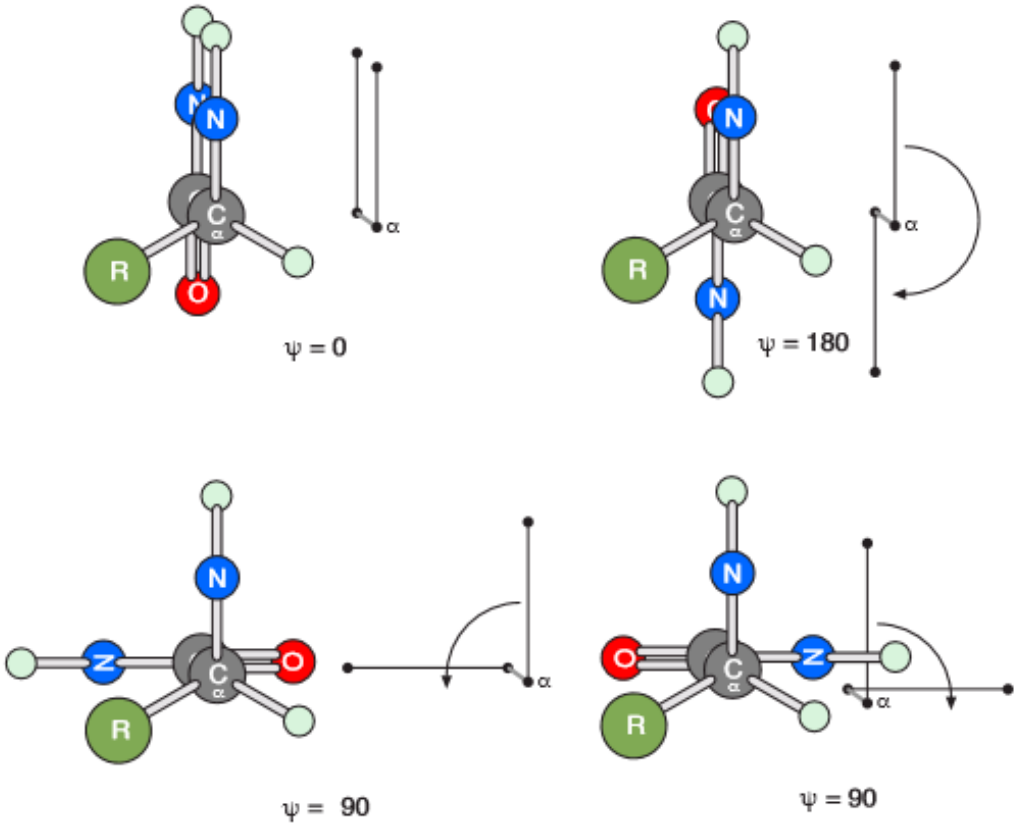

Figure 13: Rotation of psi bond looking down the alpha carbon with the carbonyl carbon at the back[29]

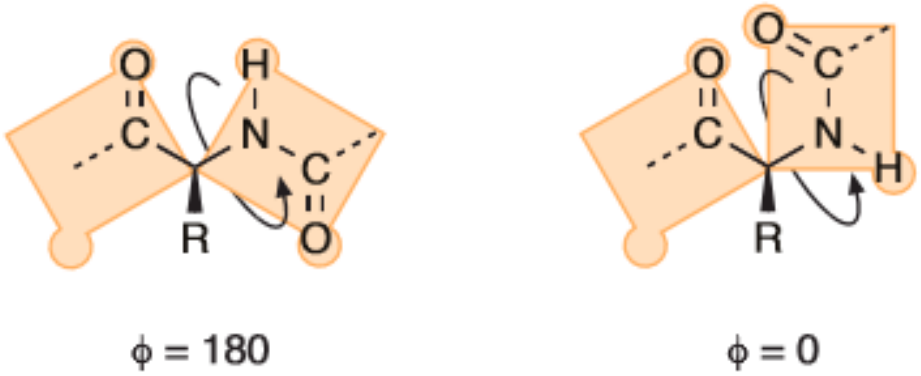

Figure 14: Rotation of phi bond[29]

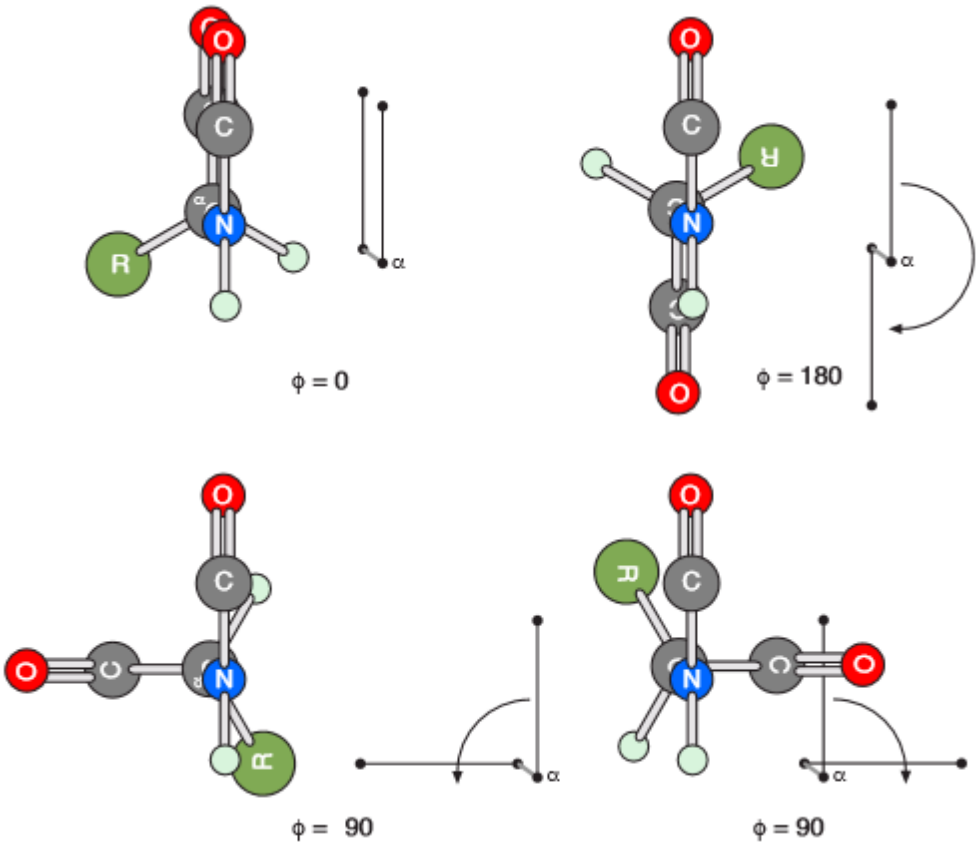

Figure 15: Rotation of phi bond looking down the amide nitrogen with the alpha carbon at the back[29]

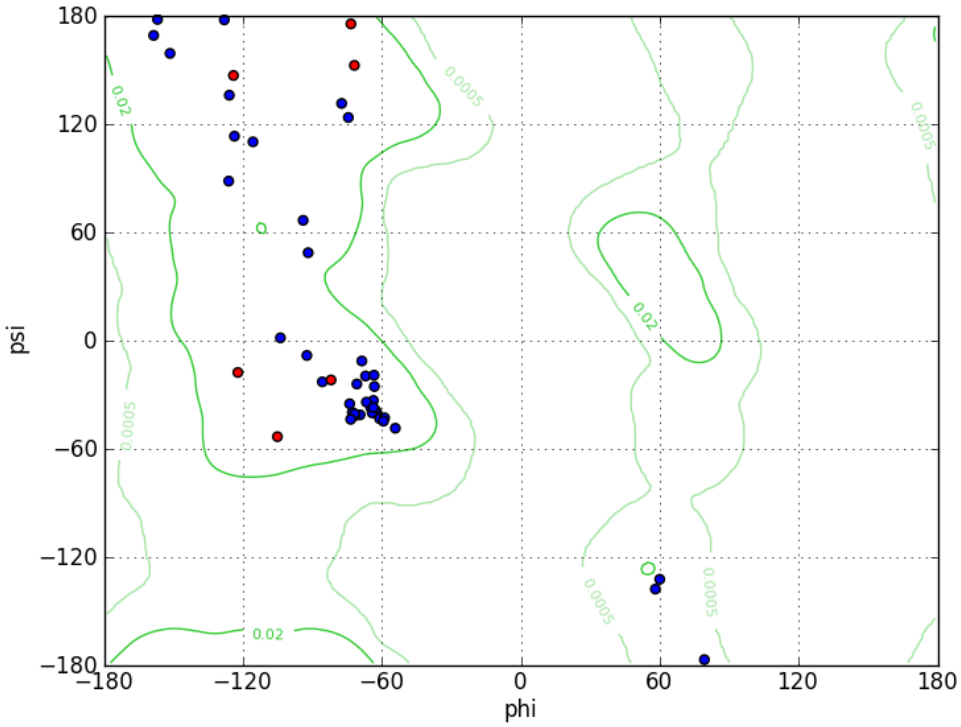

Figure 16: Ramachandran plot for bovine insulin. Cysteine residues colored red, all other residues blue. Green lines show the probability contour based on a reference set of high-resolution proteins. Graph constructed using Chimera viewing software, picking general amino acid as the probability contour (PDB file: 6QQ7, bovine insulin).

As can be seen in the Ramachandran plot above, the top three cysteine residues (A11, A20 and B7) are most likely parts of loops or turns, the less ordered tertiary structures of proteins, although the general region where they are located (high psi, negative phi) usually codes for β-sheet as the most likely structure. The bottom three cysteine residues (A6, B19 and A7) are parts of α-helices. The Ramachandran plot further supports the structure above as the more likely structure of insulin and shows that in each disulfide bond of insulin, one of the cysteines is in a turn or loop, while the other is in an α-helix, making it difficult to judge the accessibility of one disulfide bond over another. However, it is possible to deduce something from the energetically unallowable regions of the Ramachandran plot. One of such unallowable regions spans the horizontal line where ψ is between -20° and 20° [29]. This is the clash between an amide nitrogen and the hydrogen attached to another amide nitrogen. In comparison to the other steric clashes, this one is not as energetically unfavorable, yet it still provides some hinderance. The two top cysteine residues of the α-helix group in the Ramachandran plot are inside that region of N-H steric hinderance, while the bottom residue (A7) is not. This seems to propose that the A7 residue would be more stable and therefore unlikely to relieve any steric hinderance, supporting the notion that it would be the least likely to react with any gold thiolate compound. But that is only half of the disulfide bond, since gold cannot attack both sulfurs at the same time and will favor one over the other. The sulfur attacked might be chosen based on the possibility of alleviation of steric hinderance, which would make the A7 residue less likely to be attacked.

Combined with the observation that A7-B7 is the most exposed disulfide bond according to hydrophobicity considerations, the prediction that A7 is less likely to be attacked

suggests that it might be possible to reason about the accessibility of the disulfide bonds as well as the likelihood that they will be reduced. However, any sort of conclusion is beyond the scope of this discussion.

The Lees group has recently proposed that aromatic thiols with an elongated alkyl group on the aromatic ring are expected to increase interactions with the hydrophobic core of disulfide containing proteins during folding, allowing easier access to buried disulfide bonds[18]. This could be an advantage for the insulin disulfide bonds that are not as accessible as A7-B7.

Reaction Between Insulin and Dithiothreitol

From the DeCollo and Lees study it appears that they use DTT as a way to shift the equilibrium of the reaction toward reduced insulin[1]. DTT does this by reducing the aromatic disulfides formed in the interaction between insulin and an aromatic thiol back to the starting reactants. The reaction between insulin and an aromatic thiol can be seen in Figure 17 below. After the thiol reduces insulin, it forms a disulfide which, in the presence of DTT, is subsequently broken to react again with insulin. Thus, DTT is shifting the equilibrium of the reaction toward reduced insulin.

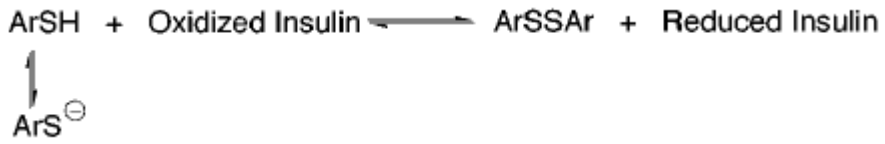

Figure 17: Reduction of insulin by aromatic thiol in the absence of DTT[1]

It is known that DTT significantly alters portions of secondary structural elements of insulin through aggregation, decreasing α-helical content from 34.8% to 13.2%,

increasing β-sheet content from 16.3% to 26.9% and random coil content from 32.3% to 42.6%[20].

In comparison to PDI, 5 to 10 times the weight of an aromatic thiol is needed to match the rate of the reduction of insulin in the presence of DTT[1]. However, PDI, the in vivo catalyst, is expensive and can be difficult to separate from other proteins, thus leaving potential for aromatic thiols to catalyze the reaction more cheaply and just as effectively[1]. It is also a possibility to use PDI and aromatic thiols congruently[12].

Arguably, DTT can also be used to reduce insulin directly, as shown by Holmgren, during which reaction DTT forms a disulfide (Figure 18). In this reaction, thioredoxin acts as the redox buffer; however, DTT reduces insulin even without a redox buffer at the expense of a reduced reduction rate.

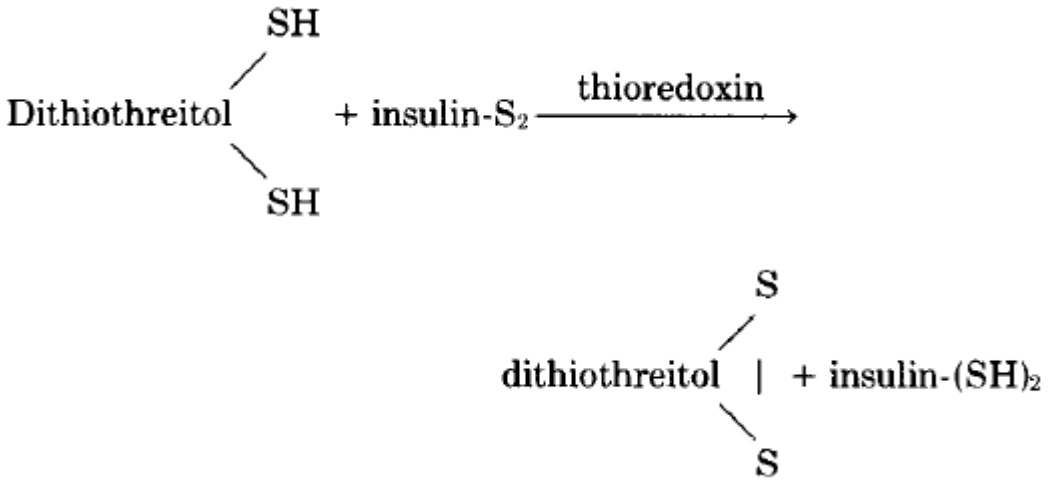

Figure 18: Formation of DTT disulfide as a result of thioredoxin catalysis[22]

An interesting application of the interactions between DTT and insulin is the percent of insulin binding to tissues that have been treated with DTT. Komori et al. showed that

binding of ^{125}I-labeled insulin to rat liver membranes increased by 21.3% after the tissues have been treated with 0.5 mM DTT[30]. Furthermore, in rat adipocyte membranes, insulin binding was increased by 107.2% when the tissues had been treated with 1.0 mM DTT[30]. Both of these experiments showed elevated receptor affinity[30]. However, in rat and human erythrocyte membranes, DTT decreased binding in a dose-dependent manner, showing a decrease in receptor affinity[30]. This has interesting implications for molecules with similar biological activities when in contact with insulin to possibly have the same effect. The importance of insulin binding activity when exposed to DTT lies in that the major event of the insulin mechanism in the body is binding to insulin receptors in tissues. If DTT is impacting the rate of binding, this change might be attributed to the aggregation of insulin by DTT.

Thiol-Disulfide Exchange

Overview

Thiol-disulfide exchange is an S_N2 reaction[31]. It is bimolecular and the rate of reaction is dependent on both reactants[31]. The first step of the reaction is a deprotonation of thiol, while the second step is the S_N2 attack of thiolate on disulfide[31]. The reaction proceeds through a transition state with a linear orientation of the three sulfur atoms[31]. A general schematic of a thiol disulfide exchange can be seen in Figure 19.

$$(1)\ HSR \rightleftharpoons {}^{-}SR + H^{+}$$
$$(2)\ {}^{-}SR + R'SSR' \rightleftharpoons {}^{-}SR' + RSSR'$$

Figure 19: Generic thiol-disulfide mechanism

Thiol-disulfide exchange is essential in structural and functional modifications that occur in many proteins[31]. The formation of mixed disulfides between glutathione or cysteine

and proteins is thought to play a role in cell signaling and regulatory pathways that are important in oxidative stress, apoptosis and aging[31].

Protein-Folding Thiol-Disulfide Exchange Reactions

When proteins are overexpressed in bacteria, they are isolated as aggregates of inactive protein known as inclusion bodies, and to obtain the active form of the protein, the inactive protein is denatured and then folded in vitro[1]. The folding of disulfide containing proteins from denatured protein to native protein involves numerous thiol-disulfide interchange reactions[1]. A number of these reactions include a redox buffer, which is a mixture of a thiol (RSH) and the corresponding disulfide (RSSR)[1]. A study conducted in 2001 by Todd DeCollo and Watson Lees concluded that aromatic thiols speed up the thiol disulfide exchange reaction between dithiothreitol (DTT) and insulin, as seen in Figure 20[1]. The proposed reason for the higher catalytic activity of the *aromatic* thiols is the similarity of their pKa to that of the in vivo catalyst, protein disulfide isomerase (PDI), with lower pKa values correlating to a higher increase in protein folding and unfolding rates[1]. It is also known that aromatic thiolates (pKa=5~6) are better leaving groups than aliphatic thiolates such as glutathione (pKa=8.7), due to their lower thiol pKa values[13]. Additionally, aromatic thiolates are better nucleophiles than aliphatic thiolates with similar thiol pKa values[13].

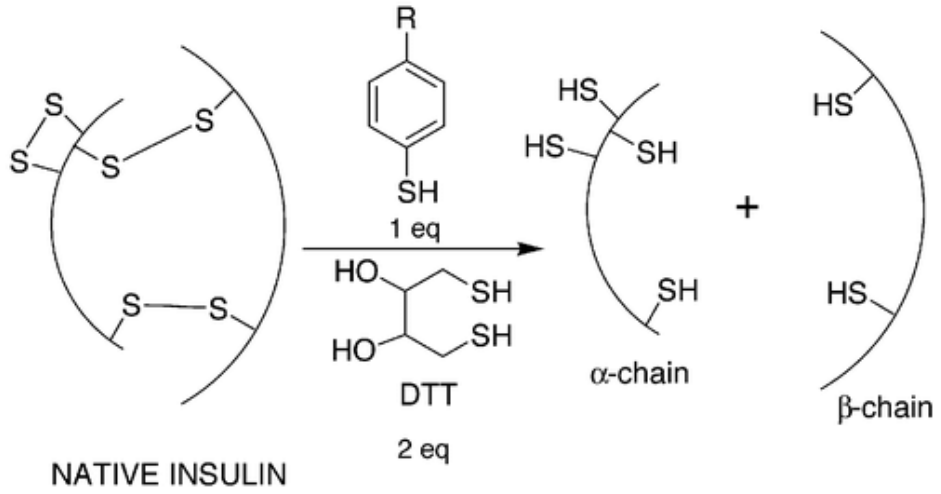

Figure 20: Reduction of native insulin by aromatic thiol and DTT at pH 6.5[1]

Using an aromatic thiol, the rate would be expected to not only increase when *folding* the protein, but in the reverse reaction as well. There are many factors that become important when studying protein folding. In many cases when proteins are overexpressed in bacteria, they are isolated as aggregates of inactive protein known as inclusion bodies[1]. To obtain the active version of the protein, the inactive protein is denatured and then folded[1]. For proteins containing disulfide bonds (such as insulin) the folding rate is usually limited by a thiol-disulfide interchange reaction. This reaction occurs in the protein itself as well as between the protein and the redox buffer, mentioned earlier[1]. The reaction occurs in the protein by breaking or forming the two disulfide bonds that hold the two peptide chains of insulin together, and it occurs between the protein and the redox buffer by breaking the disulfide bond on the outside of the alpha chain and also probably interacting with the newly formed thiolates on the inside of the two chains, as seen in Figure 21. The standard redox buffers, until the DeCollo/Lees study, were mercaptoethanol and cysteine derivatives such as glutathione[1]. As a precursor to the

study, DeCollo and Lees sought to design small molecule thiols as redox buffers for protein folding, basing their predictions on thiol pKa values and inherent nucleophilicity of PDI[1]. During their study, they found that, as stated above, aromatic thiols significantly increased the rate of reaction between DTT and insulin[1]. They also found that the two-step reduction of protein disulfides to dithiols is an important component of the folding process as it removes intermediates with mismatched disulfide bonds, as seen in Figure 21[1].

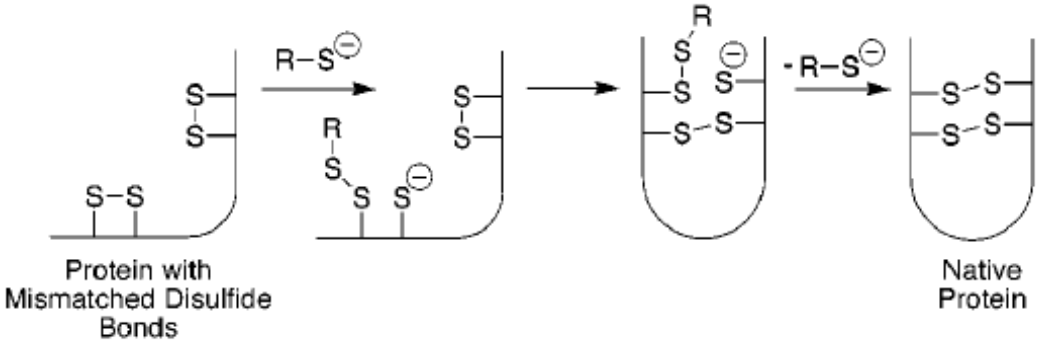

Figure 21: Folding of a protein with mismatched disulfide bonds[1]

As can be seen in the figure, instead of holding the two chains of the protein together, the mismatched disulfide bonds prevent the protein from being effective, which is problematic, since only correctly folded proteins are functional. The refolding process gains native protein, which is fully functional. Since disulfide bonds are the only covalent bonds formed during in vitro folding, their formation is usually the rate-determining step[32]. A number of factors affect the folding rate of a disulfide containing protein with an aromatic thiol, namely the concentration of thiol in the neutral RSH form, the concentration of the thiolate anion and the reactivity of the thiolate anion[13]. The concentration of thiol in the thiolate form is important because thiolate is the reactive

species in the thiolate-disulfide interchange reaction[13]. As stated above, the reactivity of the thiolate is linked to the thiolate pKa: the lower the aromatic thiolate pKa, the higher the reactivity of the thiolate, although compared to aliphatic thiols with the same pKa, the aromatic thiols are more reactive[13]. In short, the thiol must have a small pKa (be relatively acidic).

A mechanism for the refolding of insulin that was proposed by Gabor Markus predicts that the chance establishment of the first correct disulfide bond will greatly increase the chances of the formation of the next correct bond, by a) reducing the degrees of freedom available for random recombination, and by b) helping to align properly one or more additional pairs of correct sulfhydryl partners[28]. However, as insulin may interact not only with the reducing DTT but also with the RSH/RSSR buffer, the following eight reactions may be occurring during the in vitro folding of a protein disulfide[32] (Figure 22).

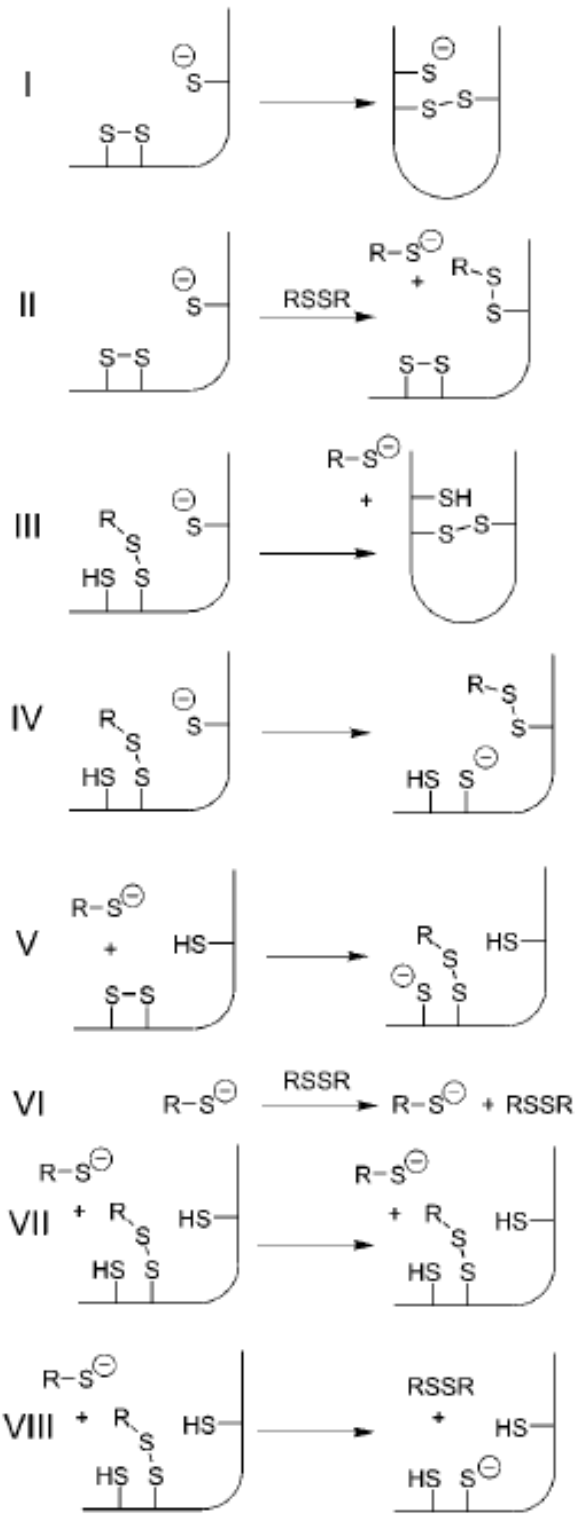

Figure 22: Eight variations of the thiol-disulfide reaction that can occur during in vitro folding of a protein disulfide with a small molecule thiol (RSH) and a small molecule disulfide (RSSR)[32]

The first four of the reactions involve the protein thiolate acting as the nucleophile, while the last four reactions have the small molecule thiolate (DTT and/or aromatic thiol and/or gold thiolate) acting as the nucleophile[32].

Optimized Conditions for Protein Folding

As found by the Lees research group, the yields of protein folding decrease with increasing protein concentration, so naturally, folding at low protein concentrations is advantageous[5]. However large amounts of refolding solution are needed to refold the protein, making it impractical on the large scale[5]. As an efficient strategy, the addition of folding aids was utilized (usually guanidine hydrochloride, urea, arginine, and glycerol)[5]. The proposed method that folding aids utilize for increasing the folding yield is by interfering with the intermolecular hydrophobic interactions that lead to protein aggregation during in vitro folding[5]. While aggregation causes reduced overall yields, folding aids are a way to increase yield, but folding aids generally decrease the rate of protein folding[5]. This is where aromatic dithiols were utilized. Aromatic dithiols were observed to increase both the rate of folding and overall yield, which has not been achieved by any other type of molecule so far[5]. Aromatic thiols are also much more cost effective compared to glutathione and PDI (aromatic thiols are about 1% the cost of glutathione)[33].

Effect of Disulfide Bond Cleavage on Biological Activity

Studies have shown that disulfide cleavage affects biological activity very drastically[23]. The half-maximal inhibition concentration for human insulin was found to be 0.71 nM (100%), while insulin mutants that had a deleted disulfide bond only had 0.2% of this activity, with some having a percentage that is even 4 to 5 times smaller than that[23]. Furthermore, the deletion of the disulfide bonds has an effect on the secondary structure of insulin[23]. Insulin contains approximately 45% α-helical content, whereas mutants with a deleted disulfide bond had anywhere from 11 to 22% α-helical content, and one had no α-helical content at all[23].

Gold Thiolate, Disulfide Exchange

Overview

The influence of gold(I) on the mechanism of thiolate, disulfide exchange was studied thoroughly over the past several years. It was found that gold(I) can indeed participate in thiolate-disulfide exchange due to several factors, such as gold(I)'s high affinity for sulfur and selenium[31]. Cellular targets for gold compounds primarily include cysteine and/or selenocysteine-containing proteins[31]. In addition, early studies have shown that gold accumulates in inflamed synovial tissues, and similarly to other heavy metals, Au(I) ions lead to expression of thionein[31]. This and other evidence cited above suggests that the gold thiolate-disulfide exchange mechanism is important and warrants further study.

The rate law for a gold thiolate-disulfide exchange reaction is overall second order, first order in gold(I)-thiolate and disulfide[31]. Electrochemical/chemical research is consistent with a mechanism involving the formation of a [Au-S,S-S], four-centered metallacycle intermediate during the exchange (Figure 23)[31].

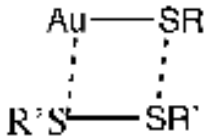

Figure 23: Four-centered metallacycle intermediate

Gold Thiolate, Disulfide Exchange Mechanism

In general, a proposed gold thiolate-disulfide exchange between insulin and either $Et_3PAuSpy$ or $Et_3PAuSba$ can be seen in Figure 24 below where the first reactant is the gold thiolate complex, the second reactant is insulin, the first product is an assumed gold thiolate-insulin complex, and the other product is a mixed disulfide formed from the thiolate ligand and the other part of the insulin that is not involved in the gold complex.

$$Et_3PAu\text{-}SR + R'SSR'' \rightarrow Et_3PAu\text{-}SR' + RSSR''$$

Figure 24: Predicted gold thiolate-disulfide exchange with an unsymmetrical disulfide

However, research has shown that gold-thiolates undergo exchange in a two-step manner, first forming an unsymmetrical disulfide and then reacting this disulfide again to produce a symmetric disulfide (Figure 25)[8,34].

$$R_3PAuSR' + R^*SSR^* \rightleftarrows R_3PAuSR^* + R^*SSR'$$

$$R_3PAuSR' + R^*SSR' \rightleftarrows R_3PAuSR^* + R'SSR'$$

Figure 25: Two-step reaction of gold-thiolate with symmetric disulfide[34].

Gold Thiolates as Disulfide Bond Cleavage Reagents

According to recent gas phase research, the high affinity of gold to sulfur suggests gold(I) complexes may prove useful as disulfide cleavage reagents[35]. Possible sites of cleavage are seen in Figure 26. It was found that disulfide bond (Figure 26 bond 1) cleavage becomes less favorable as the size of the peptide increases[35]. The fragmentation is instead dominated by amide bond (Figure 26 bonds 3 and 4) cleavage via elimination of CH_2NH_2, and no disulfide bond cleavage is observed[36]. This is because in comparison to the energetics of simple amide bond cleavage, S-S bond cleavage reactions are higher in energy[24,36]. However, out of all coinage metal systems studied, Me_3PAu^+ was superior in promoting disulfide bond cleavage (60% S-S bond cleavage, where the second highest was Ag with 10.8% S-S bond cleavage)[35].

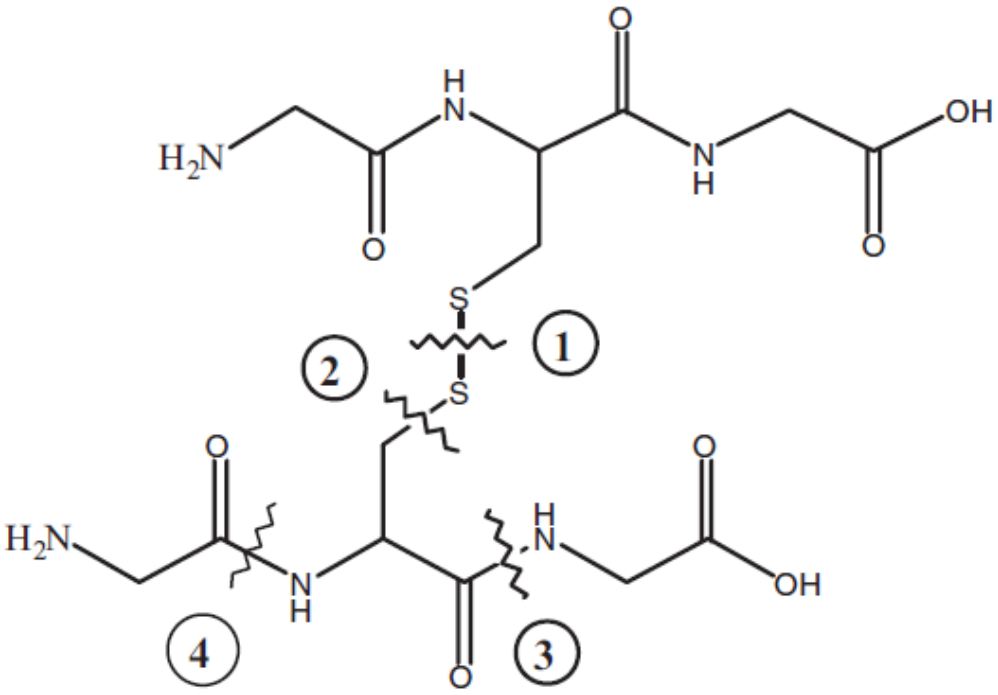

Figure 26: Possible bond cleavages in a disulfide bond between two cysteine residues[35]

A proposed electrophilic mechanism that was based on potential high S affinities and previous studies was proposed by the Lioe research group (Figure 27). In the case of insulin, one chain would form product A, while the other chain would form the cyclic byproduct, where the β-chain is expected to contain a five-membered ring at each cysteine location with the sulfur of the cysteine bound to the C-terminal amide nitrogen. This is supported by further studies[27]. It is worthwhile to point out that this mechanism is based on ionic versions of the metal complex and insulin and is also based on the method of low-energy collision-induced dissociation (CID) reactions, which provide structural information on peptides containing a disulfide bond[37].

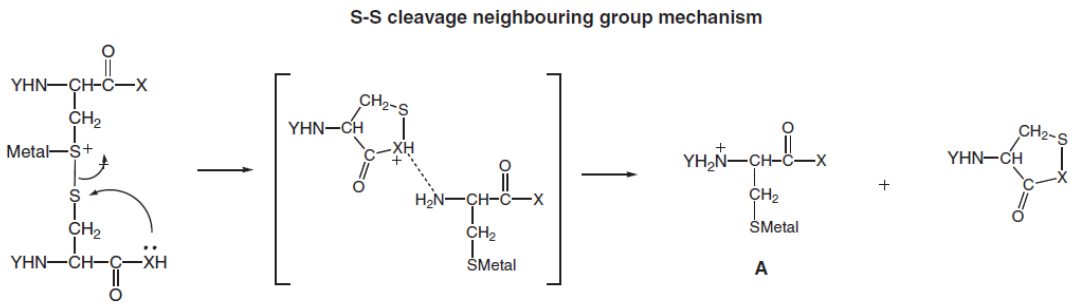

Figure 27: Proposed electrophilic neighboring group mechanism for the cleavage of disulfide bonds upon the coordination of a metal complex to one of the sulfurs of the disulfide bond. X and Y are nearby amino acids[35].

Proteins as a Mode of Transport for Gold Thiolate Compounds

It is known that upon entering the body, Au(I) becomes bonded to cysteine sites in glutathione, blood proteins and enzymes and is extensively distributed around the body while undergoing rapid ligand displacement reactions[8,38]. It is known that most of the circulating Au from antiarthritic drugs is bound to the cysteine-34 of serum albumin (pKa~5) and transcription factors (Jun, Fos, NF-kB), which have cysteine residues flanked by basic lysine and arginine residues[2]. Albumin can transfer Au(I) into cells via a

thiol shuttle mechanism[7]. When a phosphine gold ligand binds to Cys-34 of albumin, it flips the cysteine residue from the buried pocket of albumin to the surface, where it is more readily accessible (Figure 28)[39].

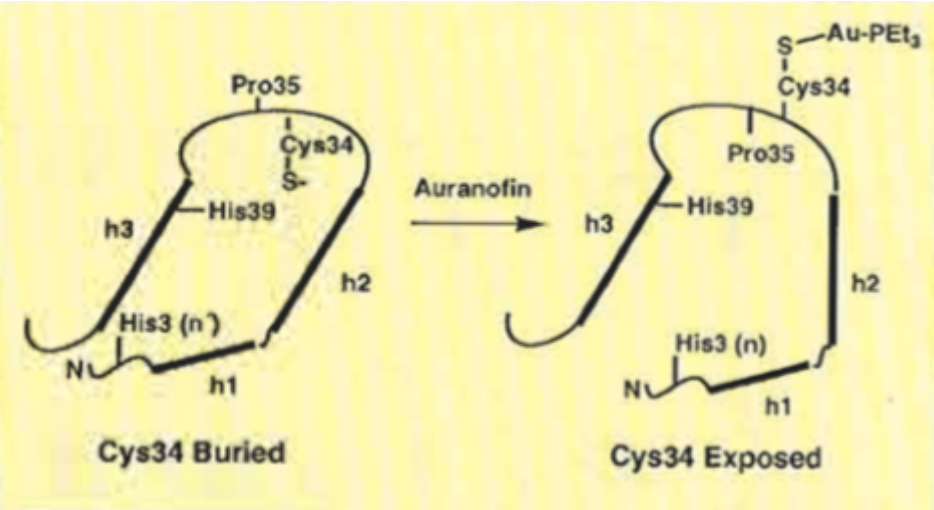

Figure 28: Structural transition induced by Au(I) in serum albumin[39].

Since most gold drugs release the Et_3PAu^+ moiety *in vivo*, the other attachment in the complex could potentially regulate the permeability into the cell and the ease of transport.

Gold Thiolate as Redox Buffer

If the formation of the DTT disulfide in this reaction is possible, then it is also possible that an aromatic thiol or a gold thiolate could interact with DTT in the same way that DTT interacts with aromatic thiols, namely a gold thiolate could be used to reduce the DTT disulfide and shift the equilibrium of the reaction toward reduced disulfide. However, phosphine gold(I) thiolate complexes have been shown to react with aromatic disulfides via two pathways: 1) thiolate-disulfide exchange and 2) pathway that leads to the formation of phosphine oxide[34]. These pathways are in competition. If gold thiolates

are reacting with aromatic disulfides, it could be possible that they may be reacting with DTT disulfides after DTT reduces insulin.

METHODS

Materials

Insulin (bovine, ≥ 25 USP units/mg (HPLC), powder) and K_2HPO_4 were acquired from Alfa Aesar. Dithiothreitol (DTT) was acquired from Fluka BioChemika and Acros Organics. Et_3PAuCl, Trizma, d-Chloroform, DMSO, 4-mercaptobenzoic acid and 2-mercaptopyridine were acquired from Sigma-Aldrich. EDTA, KH_2PO_4, HCl, and NaOH were acquired from Fischer Scientific. Ethanol was acquired from Pharmco-Aaper. $Et_3PAuSpy$ and $Et_3PAuSba$ were both synthesized in lab.

Preparation of insulin stock solution # 1[22]

To prepare a 10 mg/mL insulin stock solution, 0.0250 g of bovine insulin was dissolved in 4 mL of 0.05 M Tris-Cl buffer, pH 8.00, and adjusted to pH 2 by the addition of 1 M HCl and rapidly titrated back to pH 8 with 1 M NaOH (about 4 drops each of HCl and NaOH). The solution was then adjusted to 5 mL total volume with distilled water. The stock solution was stored at freezing temperature.

Preparation of insulin stock solution # 2[1]

To prepare a 0.167 mM insulin stock solution, 1 mL of a 10 mg/mL solution of insulin (stock solution 1) was diluted to 8 ml with 0.1 M phosphate buffer. This cloudy solution was made clear by adjusting to pH 3 by adding 1 M HCl dropwise and then rapidly adjusting to pH 8 by adding 1 M NaOH dropwise. The final volume of insulin was adjusted to 10 mL with distilled water. The stock solution was stored at freezing temperature.

RESULTS AND DISCUSSION

Each experiment contains a Methods section and a Results and Discussion section. It seems more convenient to use this method of organization so that the reader can refer to the components of the reaction vessel when reading the results and discussion.

Table 1: List of experiments, reactants and final concentrations in cuvette (mM). All experiments conducted in a buffer were at pH 6.5 (buffer pH). Insulin's pH is 8.

Experiment Name	**Reactants**	**Final Concentration in Cuvette (mM)**
A	4-mercaptobenzoic acid, DTT, insulin	0.266, 0.333, 0.0556
B	DTT, insulin	0.333, 0.0556
C	4-mercaptobenzoic acid, insulin	0.266, 0.0556
D	2-mercaptopyridine, DTT, insulin	0.266, 0.333, 0.0556
E	$Et_3PAuSpy$, DTT, insulin	0.266, 0.333, 0.0556
F	$Et_3PAuSpy$, insulin	0.266, 0.0556
G	$Et_3PAuSpy$, DTT	varied (titration)
H	Et_3PAuCl, insulin	0.266, 0.0556
I	Et_3PAuCl, DTT	0.266, 0.333

Experiment A (4-mercaptobenzoic acid, DTT and insulin)

Methods: To prepare 20 mL of a 5.0 mM 4-mercaptobenzoic acid solution, 0.0154 g (0.0999 mmol) were dissolved in 20 mL of phosphate buffer. The solution was stirred and heated until all of the solid was dissolved in the solution. To prepare 20 mL of a 25.0 mM dithiothreitol solution, 0.0778 g (0.504 mmol) were dissolved in 20 mL of phosphate buffer. The solution was stirred until all of the solid was dissolved in the solution. Insulin stock solution 2 was warmed to room temperature. The UV-Vis was autozeroed on phosphate buffer, not air. To make the cuvette solution, 1 mL of insulin stock solution 2 was added to the cuvette, followed by 1.8 mL of phosphate buffer, 160.0 μL of 4-

mercaptobenzoic acid solution and 40.0 µL of dithiothreitol solution. The UV-Vis was set up to scan the cuvette every 3 minutes (including the 25 sec it takes to actually perform a scan) in the wavelength range of 300-800 nm. The total number of scans was 283 (approx. 14 hrs). The absorbance at 650 nm as a function of time in minutes was plotted in Figure 29.

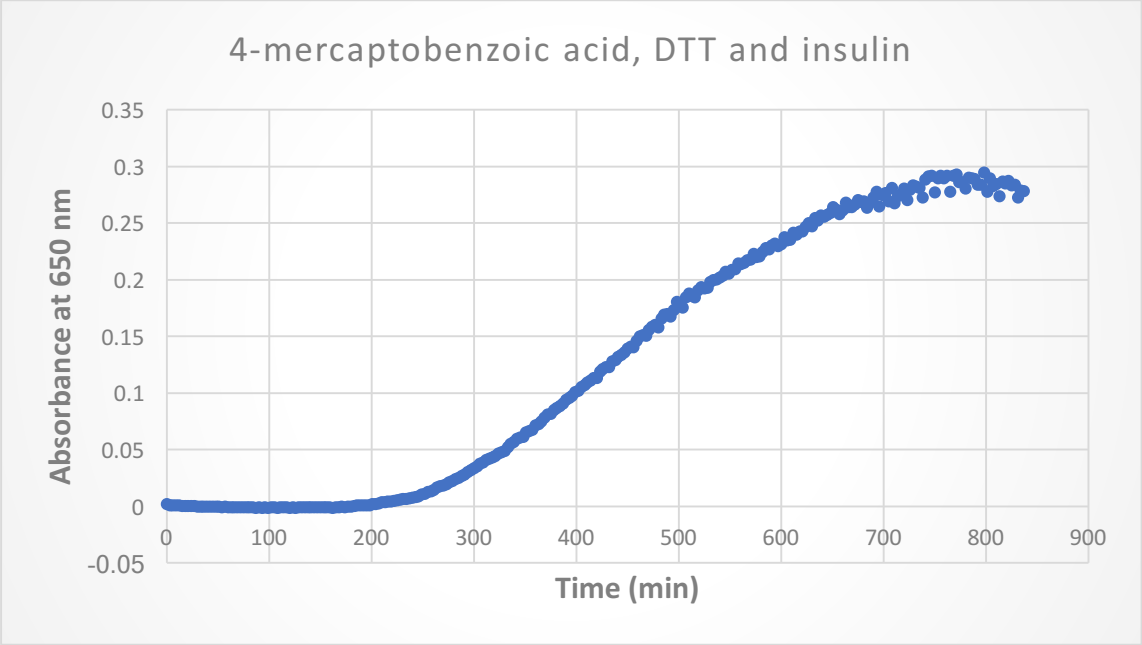

Figure 29: Absorbance at 650 nm plotted as a function of time of the reaction between 4-mercaptobenzoic acid, DTT and insulin. Graph shows the formation of a colloidal suspension of the α and β chains precipitating out of solution. The plot shows a lag time, during which the particles are predicted to be reaching a critical concentration and start aggregating after reaching it (200 min). Upon reaching the maximum size of the aggregate, the particles start falling out of solution, becoming too dense to form a colloidal suspension. This is evidenced by the decrease in light scatter at 820 min.

Results and Discussion: This experiment was carried out as a proof of concept of the procedure for a thiol-mediated DTT reduction of insulin described by DeCollo and Lees[1]. Because of a different total volume of this reaction from theirs (their total volume was 1.2 mL, while the total volume of the experiments in this study was 3 mL), the concentrations of the reactants in this experiment differed from theirs, although the molar ratio was the same. In terms of a proof of concept, the reaction was a success, since there was a colloidal suspension forming in the cuvette with time, increasing the light scatter until the particles become too dense for the solution and begin falling. As reported by Holmgren, there is a considerable lag time that occurs before the precipitation of the chains in solution[22], in this case, approximately 3 hours. A proposed mechanism for the reaction between 4-mercaptobenzoic acid, insulin and DTT can be seen in Figure 30.

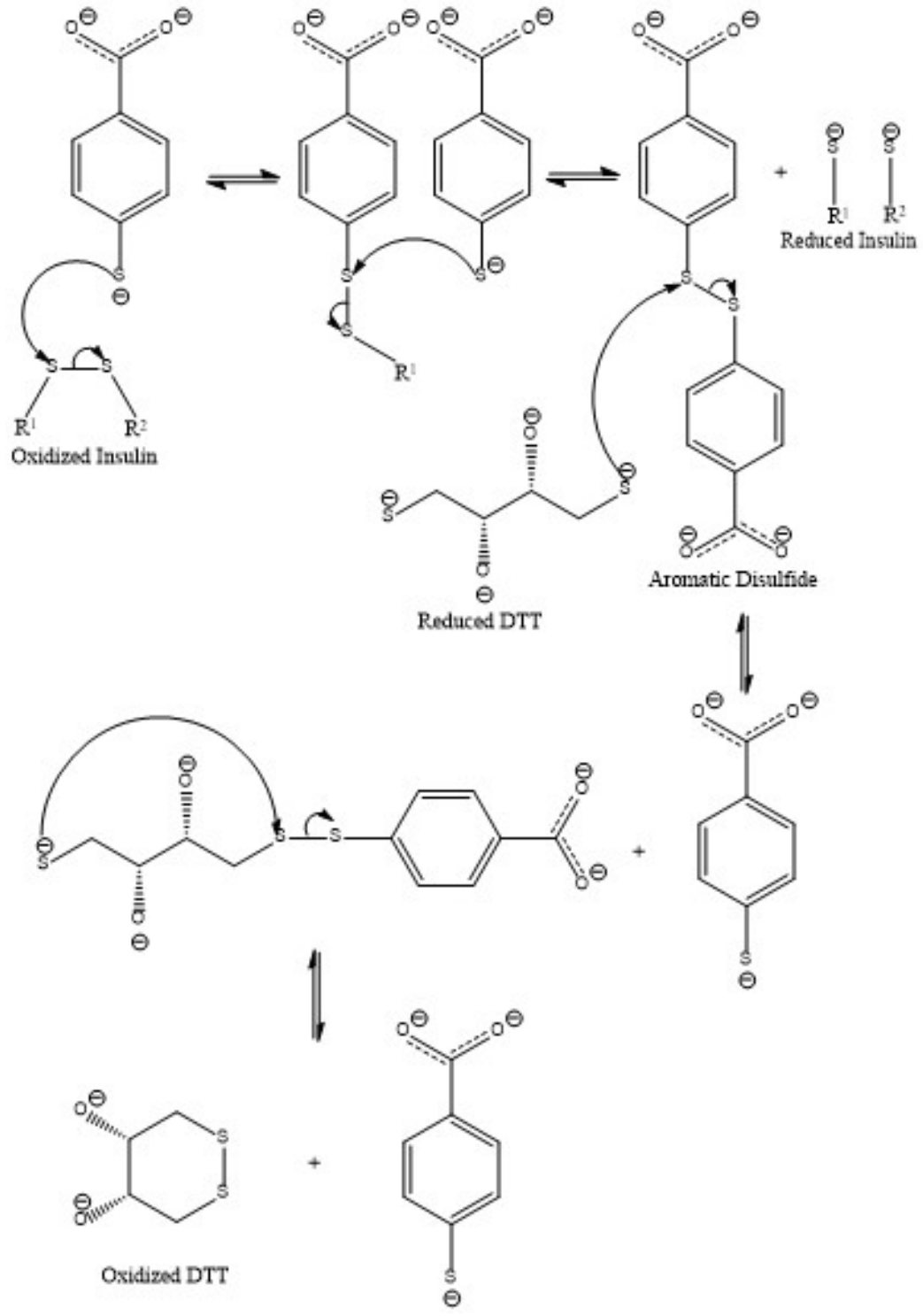

Figure 30: Proposed mechanism for the reaction between 4-mercaptobenzoic acid, insulin and DTT, where R^1 and R^2 are the α and β chains of insulin. DTT acts as a redox buffer, breaking the aromatic disulfide to provide more 4-mercaptobenzoic acid to reduce insulin, thereby shifting the equilibrium of the reaction toward reduced insulin. 4-mercaptobenzoic acid also acts as a redox buffer.

Experiment B (DTT and insulin)

Methods: To prepare 20 mL of a 25.0 mM dithiothreitol solution, 0.0777 g (0.504 mmol) were dissolved in 20 mL of phosphate buffer. The solution was stirred until all of the solid was dissolved in the solution. Insulin stock solution 2 was warmed to room temperature. The UV-Vis was autozeroed on phosphate buffer, not air. To make the cuvette solution, 1 mL of insulin stock solution 2 was added to the cuvette, followed by 1.96 mL of phosphate buffer and 40.0 µL of dithiothreitol solution. The UV-Vis was set up to scan the cuvette every 3 minutes (including the 25 sec it takes to actually perform a scan) in the wavelength range of 300-800 nm. The total number of scans was 502 (approx. 25 hrs). The absorbance at 650 nm as a function of time in minutes was plotted in Figure 31.

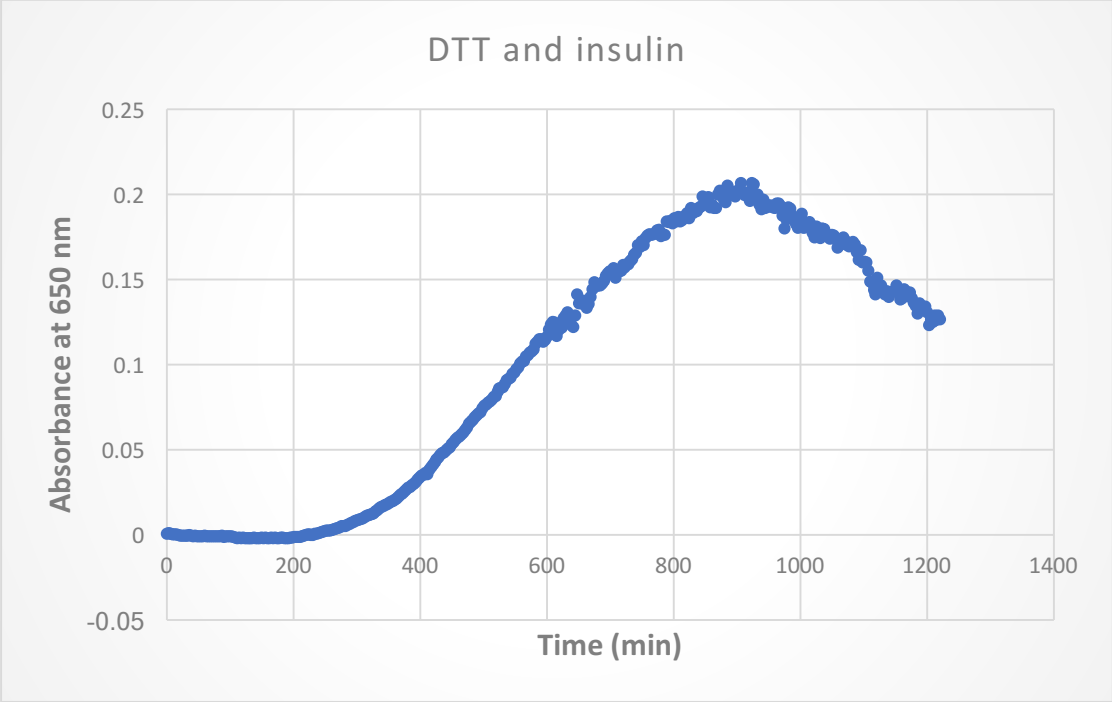

Figure 31: Absorbance at 650 nm plotted as a function of time of the reaction between DTT and insulin.

Results and Discussion: This experiment was also done as a second proof of concept, as DeCollo and Lees had carried out the reaction between DTT and insulin in order to compare this reaction to the reaction of DTT and insulin in the presence of an aromatic thiol in terms of relative rates. The comparison between Experiments A and B can be seen in Figure 33 and the relative rates can be seen as the slope of the linear fit on the linear segment of both curves in Figure 34. The relative rate of experiment A is roughly 1.7 times that of experiment B, consistent with the results found by DeCollo and Lees, that aromatic thiols increase the rate of the reduction of insulin by DTT. Lees reported a relative rate of 1.6 between the reaction of 4-mercaptobenzoic acid, insulin and DTT relative to insulin and DTT only[1]. A proposed mechanism for the reaction between DTT and insulin can be seen in Figure 32.

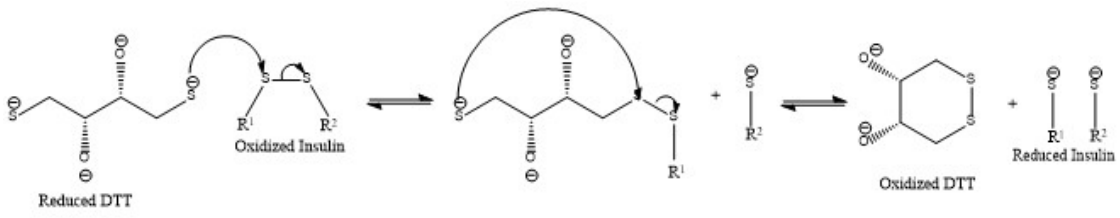

Figure 32: Proposed mechanism for the reaction between insulin and DTT, where R^1 and R^2 are the α and β chains of insulin.

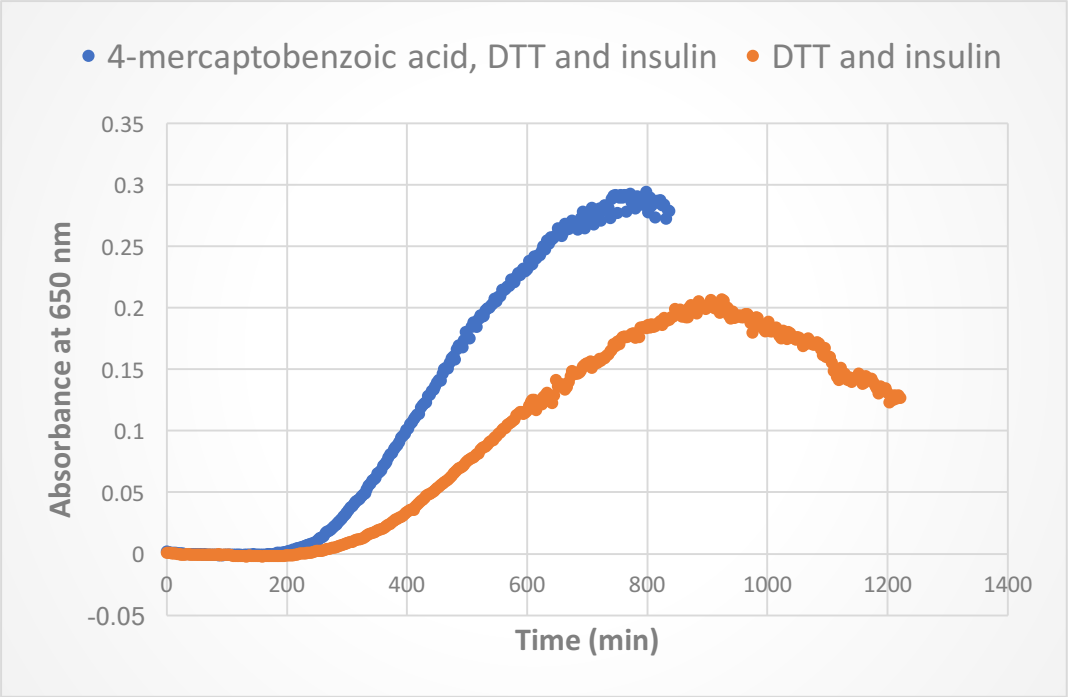

Figure 33: Comparison between Experiment A (4-mercaptobenzoic acid, DTT and insulin) and Experiment B (DTT and insulin)

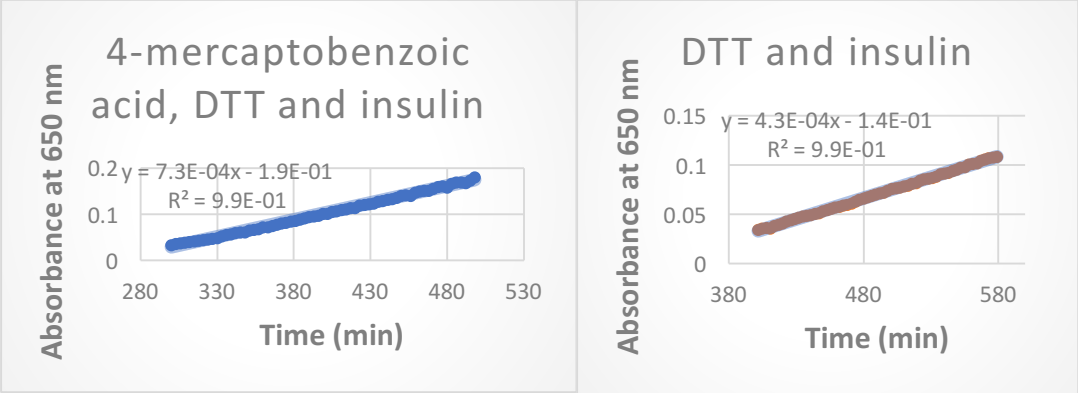

Figure 34: Comparison of the relative rates of Experiments A (4-mercaptobenzoic acid, DTT and insulin) and B (DTT and insulin), where the linear range for Experiment A is 300-500 min and the linear range for experiment B is 400-580 min.

Experiment C (4-mercaptobenzoic acid and insulin)

Methods: To prepare 20 mL of a 5.0 mM 4-mercaptobenzoic acid solution, 0.0154 g (0.0999 mmol) were dissolved in 20 mL of phosphate buffer. The solution was stirred and heated until all of the solid was dissolved in the solution. Insulin stock solution 2 was warmed to room temperature. The UV-Vis was autozeroed on phosphate buffer, not air. To make the cuvette solution, 1 mL of insulin stock solution 1 was added to the cuvette, followed by 1.86 mL of phosphate buffer and 160.0 μL of 4-mercaptobenzoic acid solution. The UV-Vis was set up to scan the cuvette every 3 minutes (including the 25 sec it takes to actually perform a scan) in the wavelength range of 300-800 nm. The total number of scans was 483 (approx. 24 hrs).

Results and Discussion: This reaction was carried out over the course of 24 hours and showed no result in the form of an increase in light scatter, suggesting either that there is no reaction between 4-mercaptobenzoic acid and insulin or that it has a significantly reduced rate and therefore has a considerably long lag time. Lees does not report the relative rates of this experiment to others.

Changing the Thiol

During synthesis of the proposed $Et_3PAuSba$ compound, to be used in later studies, it was found that the compound is not soluble in phosphate buffer. This undermines the experiment as the compound will precipitate out of solution when put in the cuvette for a reaction. Instead, it was proposed to switch the thiol from 4-mercaptobenzoic acid to 2-mercaptopyridine, since $Et_3PAuSpy$ was known to be at least partially soluble in phosphate buffer.

Experiment D (2-mercaptopyridine, DTT and insulin)

Methods: To prepare 20 mL of a 5 mM solution of 2-mercaptopyridine, 0.0216 g (0.194 mmol) were dissolved in 20 mL of buffer. The solution was stirred until all of the solid was dissolved in the solution. To prepare 20 mL of a 25.0 mM dithiothreitol solution, 0.0768 g (0.498 mmol) were dissolved in 20 mL of phosphate buffer. The solution was stirred until all of the solid was dissolved in the solution. Insulin stock solution 2 was warmed to room temperature. The UV-Vis was autozeroed on phosphate buffer, not air. To make the cuvette solution, 1 mL of insulin stock solution 2 was added to the cuvette, followed by 1.8 mL of phosphate buffer, 160.0 μL of 2-mercaptopyridine solution and 40.0 μL of dithiothreitol solution. The UV-Vis was set up to scan the cuvette every 3 minutes (including the 25 sec it takes to actually perform a scan) in the wavelength range of 300-800 nm. The total number of scans was 243 (approx. 12 hrs). The absorbance at 650 nm as a function of time in minutes was plotted in Figure 35.

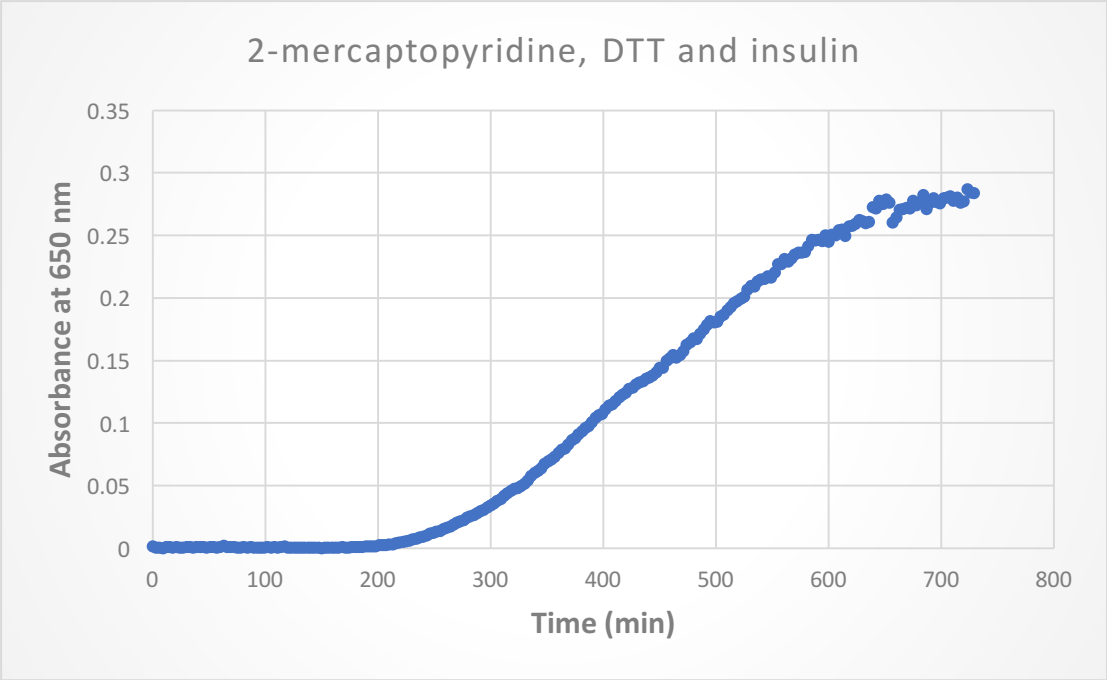

Figure 35: Absorbance at 650 nm plotted as a function of time of the reaction between 2-mercaptopyridine, DTT and insulin.

Results and Discussion: This reaction was compared to Experiment A, as the only change from Experiment A to D was the switch of the thiol used in the experiment. The comparison can be seen in Figure 36. The new thiol (2-mercaptopyridine) seems to be catalyzing the reduction of insulin by DTT in the same manner, and so is a viable substitute. The proposed mechanism for the reaction between 2-mercaptopyridine, DTT and insulin can be seen in Figure 37. The mechanism is based on the known mechanism for Experiment A, substituting the 4-mercaptobenzoic acid for 2-mercaptopyridine, which has been shown in Figure 36 to have the same effect on the reaction between insulin and DTT.

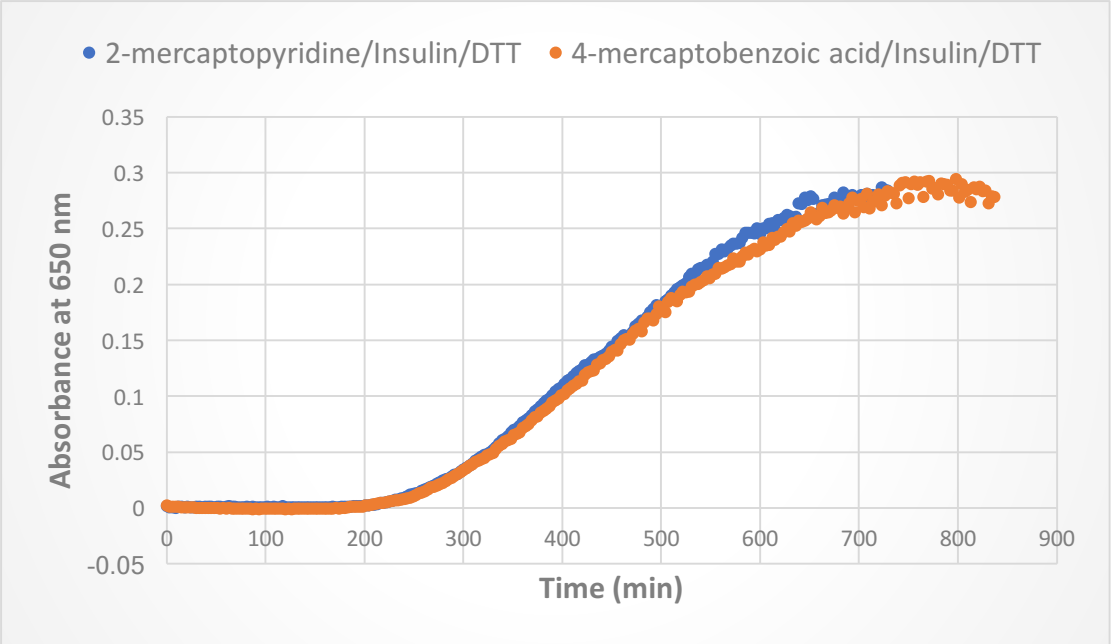

Figure 36: Comparison between Experiment A (4-mercaptobenzoic acid, DTT and insulin) and Experiment D (2-mercaptobenzoic acid, DTT and insulin).

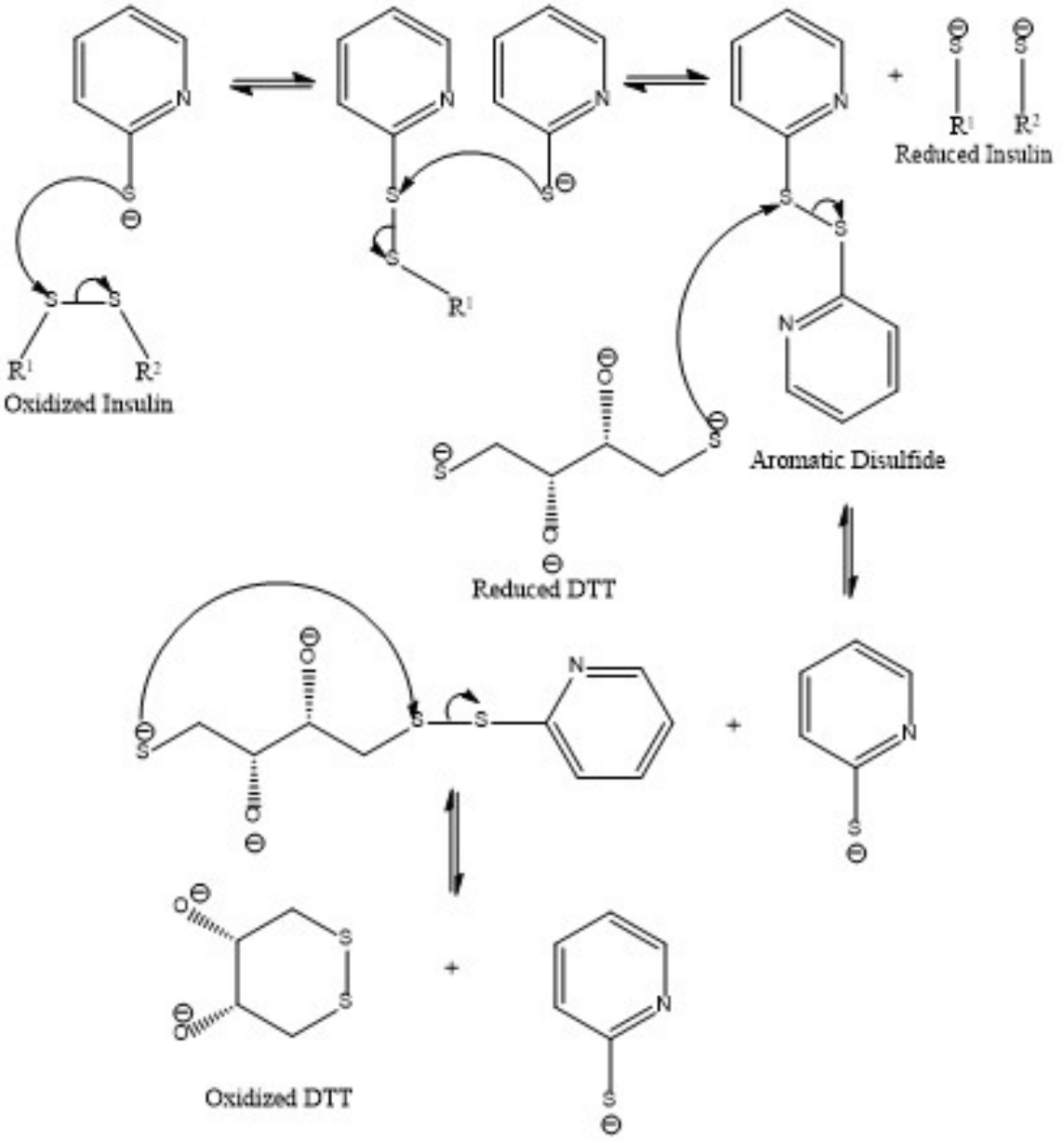

Figure 37: Proposed mechanism between 2-mercaptopyridine, insulin and DTT, where R^1 and R^2 are the α and β chains of insulin. DTT acts as a redox buffer, breaking the aromatic disulfide to provide more 2-mercaptopyridine to reduce insulin, thereby shifting the equilibrium of the reaction toward reduced insulin. The two thiols of DTT act as an oxidation-reduction couple, in the same way as PDI's two active site cysteine residues act together[40].

Experiment E ($Et_3PAuSpy$, DTT and insulin)

Methods: To prepare 1 mL of a 5.0 mM $Et_3PAuSpy$ solution, 0.0021 g (0.0049 mmol) were dissolved in 0.2 mL of dimethyl sulfoxide and diluted to 1 mL with phosphate buffer. The solution was stirred until all of the solid was dissolved in the solution. To prepare 20 mL of a 25.0 mM dithiothreitol solution, 0.0781 g (0.5063 mmol) were dissolved in 20 mL of phosphate buffer. The solution was stirred until all of the solid was dissolved in the solution. Insulin stock solution 2 was warmed to room temperature. The UV-Vis was autozeroed on phosphate buffer, not air. To make the cuvette solution, 1 mL of insulin stock solution 2 was added to the cuvette, followed by 1.8 mL of phosphate buffer, 160.0 µL of $Et_3PAuSpy$ solution and 40.0 µL of dithiothreitol solution. The UV-Vis was set up to scan the cuvette every 3 minutes (including the 25 sec it takes to actually perform a scan) in the wavelength range of 300-800 nm. The total number of scans was 273 (approx. 14 hrs). The absorbance at 650 nm as a function of time in minutes was plotted in Figure 38.

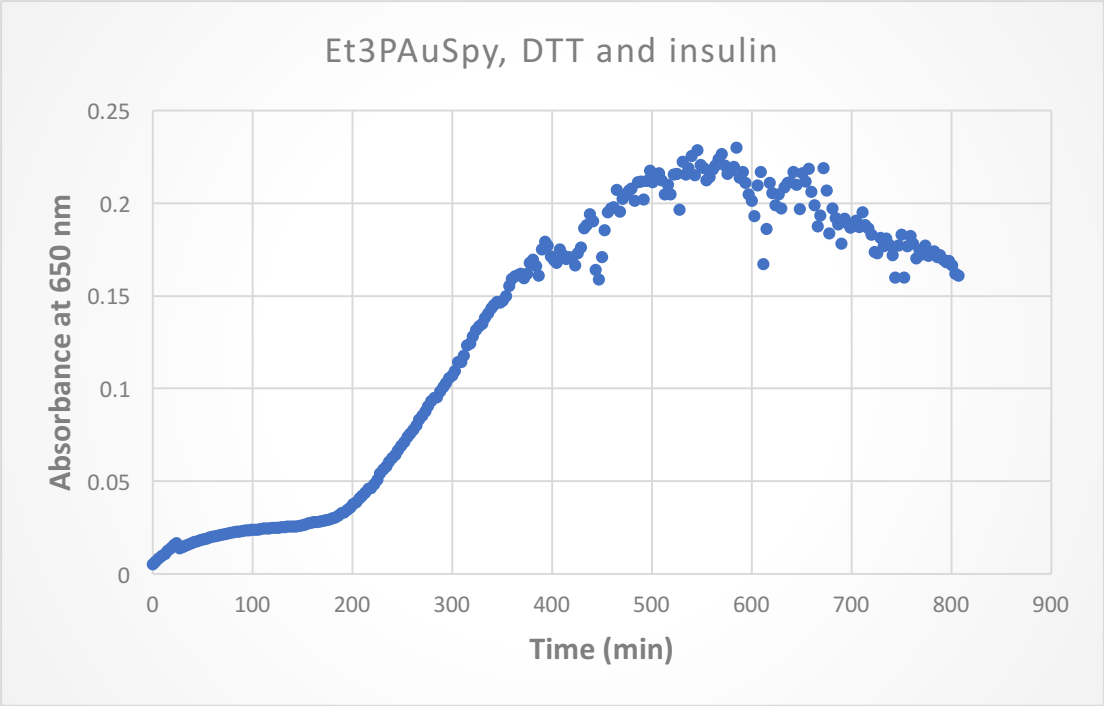

Figure 38: Absorbance at 650 nm plotted as a function of time of the reaction between $Et_3PAuSpy$, DTT and insulin.

Results and Discussion: This experiment was carried out to see if replacing a thiol with a gold thiolate would have the same effect in terms of increasing the rate of the reaction between DTT and insulin. It appears that $Et_3PAuSpy$ increases the rate of the reaction between insulin and DTT more so than 2-pyridinethiol (Figure 40). In order to compare the effect $Et_3PAuSpy$ has on the reaction, the comparison between Experiment B and Experiment E needs to be made (Figure 41). As can be seen in this graph, $Et_3PAuSpy$ considerably reduces the lag time of the reaction, as well as noticeably increasing the rate.

Similar to how DTT shifted the equilibrium toward reduced insulin when an aromatic thiol was combined with insulin in the presence of DTT, it is possible that DTT has the same function in this experiment (see Figure 43).

The offset in the two slopes in Figures 40 and 41 is most likely due to the possibility of two separate mechanisms that form different kinds of particles that aggregate at different rates. This supposition is based on the knowledge that $Et_3PAuSpy$ reacts with DTT to form 2-pyridinethiol (Experiment G) and the knowledge that $Et_3PAuSpy$ also reacts with insulin to form a colloidal suspension that scatters light at 650 nm (Experiment F). These results suggest an explanation for the initial increase in light scatter, followed by a lag time and then again an increase until reaching a maxima in the graph of Figure 38, which shows the reaction between $Et_3PAuSpy$, DTT and insulin.

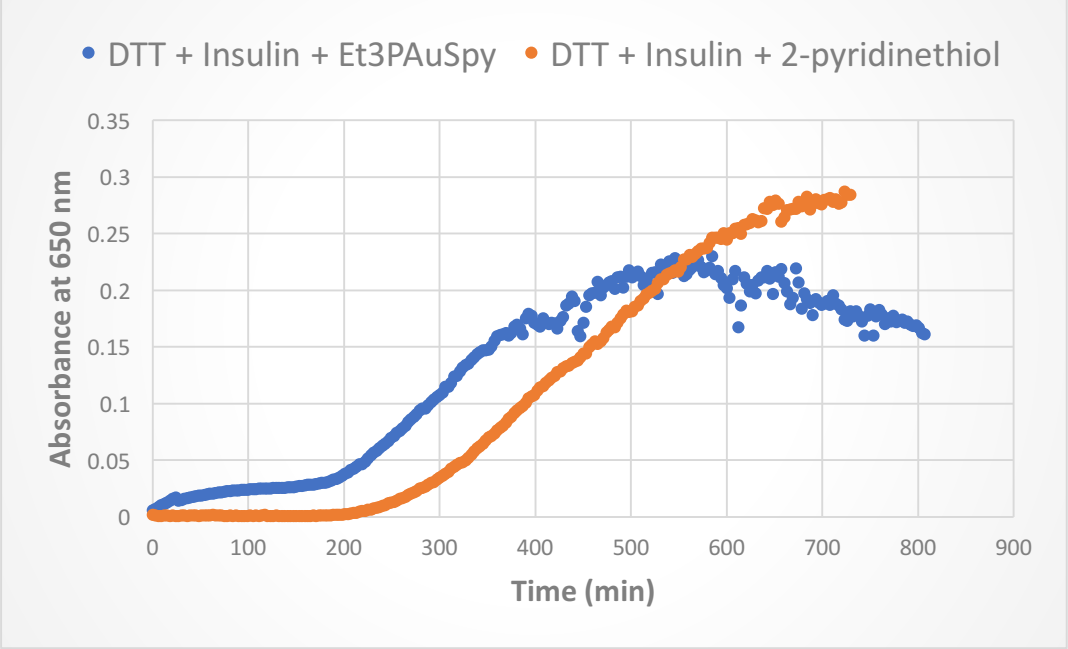

Figure 40: Comparison between experiments D (2-pyridinethiol, DTT and insulin) and E ($Et_3PAuSpy$, DTT and insulin)

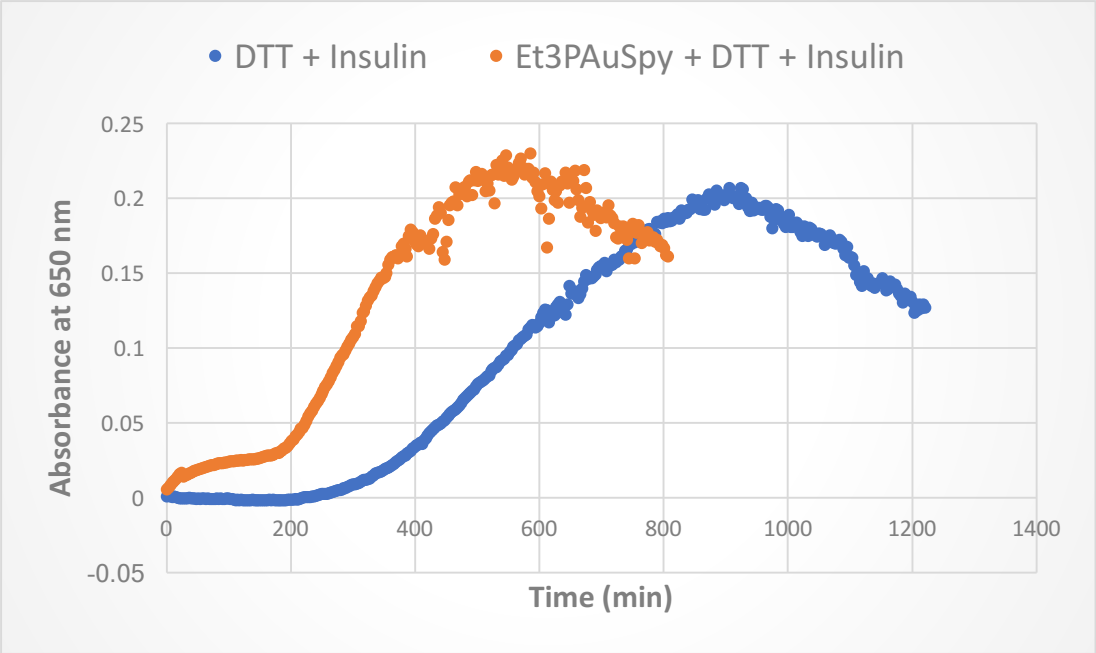

Figure 41: Comparison between experiments B (DTT and insulin) and E ($Et_3PAuSpy$, DTT and insulin)

Experiment F (Et3PAuSpy and insulin)

Methods: To prepare 1 mL of a 5.0 mM $Et_3PAuSpy$ solution, 0.0021 g (0.0049 mmol) were dissolved in 0.2 mL of dimethyl sulfoxide and diluted to 1 mL with phosphate buffer. The solution was stirred until all of the solid was dissolved in the solution. Insulin stock solution 2 was warmed to room temperature. The UV-Vis was autozeroed on phosphate buffer, not air. To make the cuvette solution, 1 mL of insulin stock solution 2 was added to the cuvette, followed by 1.86 mL of phosphate buffer and 160.0 µL of $Et_3PAuSpy$ solution. The UV-Vis was set up to scan the cuvette every 3 minutes (including the 25 sec it takes to actually perform a scan) in the wavelength range of 300-800 nm. The total number of scans was 241 (approx. 12 hrs). The absorbance at 650 nm as a function of time in minutes was plotted in Figure 42.

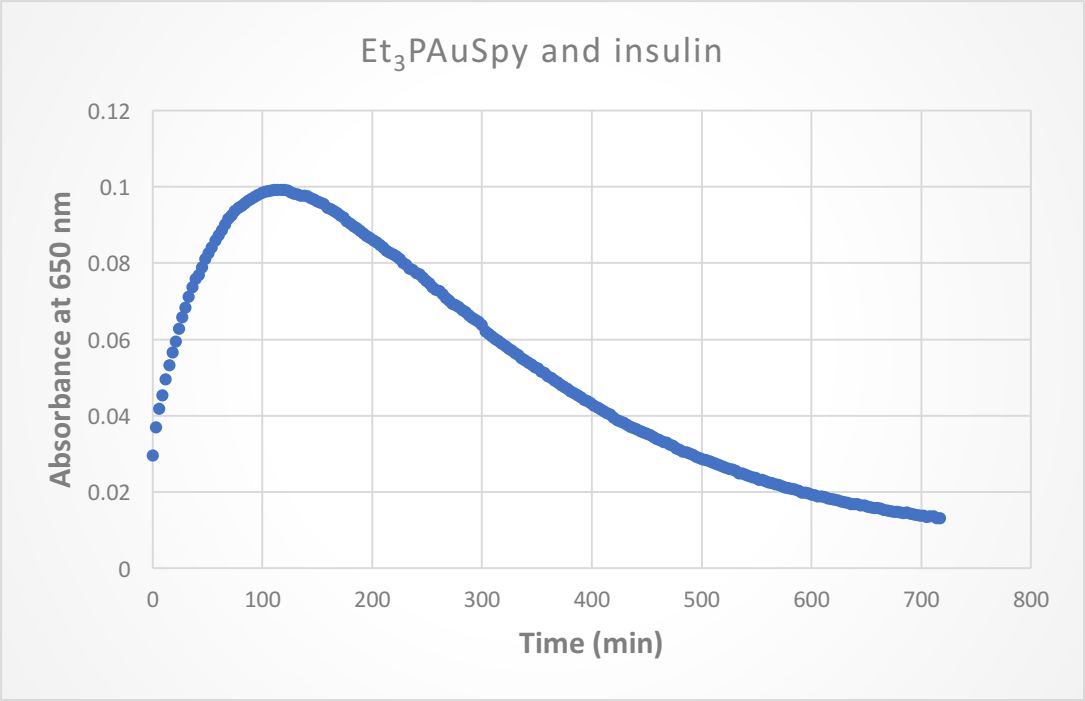

Figure 42: Absorbance at 650 nm plotted as a function of time of the reaction between $Et_3PAuSpy$ and insulin

Results and Discussion: This experiment was carried out to control for DTT. If insulin reacts with $Et_3PAuSpy$ itself, without needing DTT as a reducing agent, then the mechanism of the reaction gets more complicated, proposing the idea that there is more than one reaction happening when $Et_3PAuSpy$, DTT and insulin are mixed together. As can be seen in Figure 42, insulin does react with $Et_3PAuSpy$, and at a noticeably faster rate than the other reactions that have been investigated in this study. In comparison to the reaction *with* DTT, the reaction *without* DTT is much faster (Figure 44). The proposed mechanism for this reaction can be seen in Figure 43. The mechanism is based on the knowledge that gold-sulfur compounds undergo thiolate-disulfide exchange by forming a metallacycle intermediate with a disulfide. The shape of the graphs in Figure

44 is very different, with drastically different maxima, possibly indicating that the size of the particles grows more rapidly with gold.

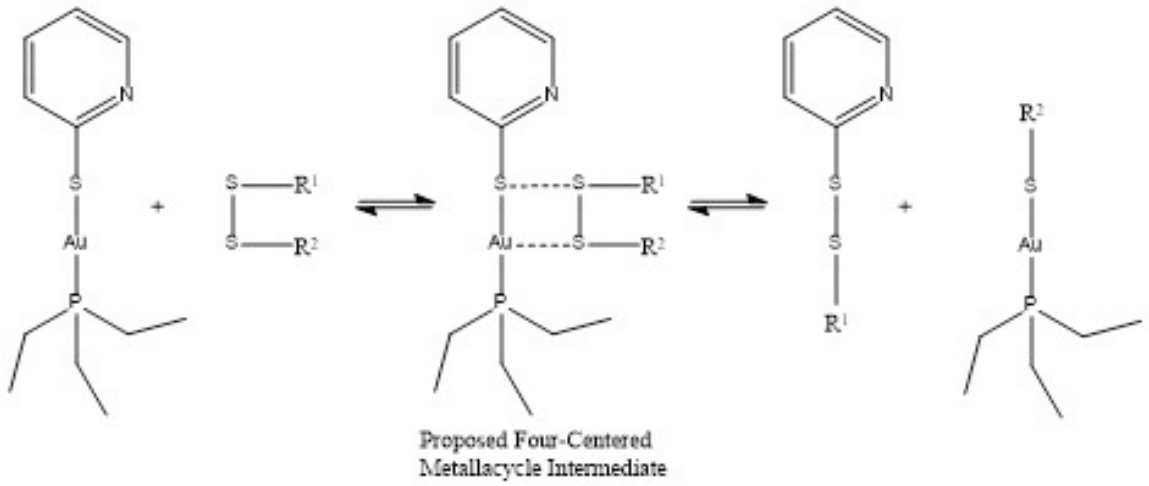

Figure 43: Proposed mechanism for the reaction between $Et_3PAuSpy$ and insulin, where R^1 and R^2 are the α and β chains of insulin.

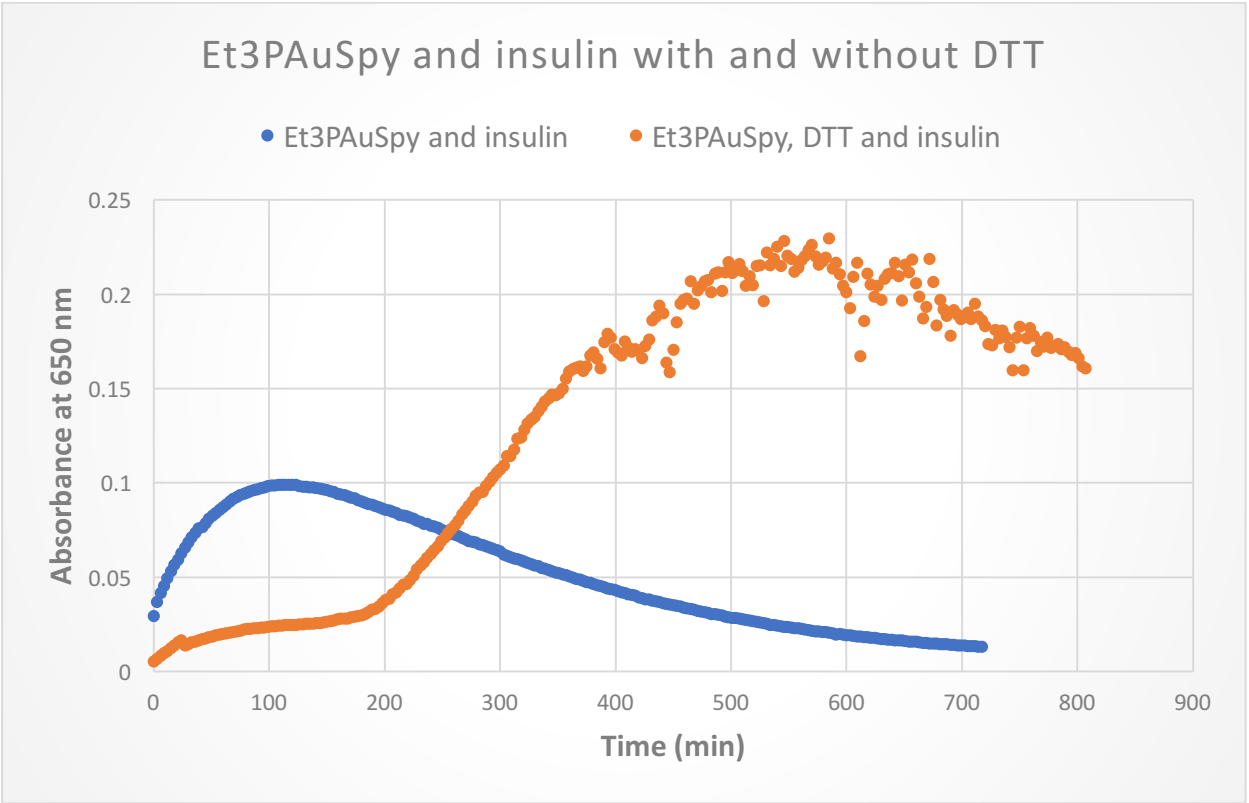

Figure 44: Comparison of experiments E ($Et_3PAuSpy$, DTT and insulin) and F ($Et_3PAuSpy$ and insulin)

Experiment G ($Et_3PAuSpy$ and DTT)

UV-Vis:

Method: To prepare 10 mL of 3 mM solution of dithiothreitol, 0.0048 g (0.0311 mmol) were dissolved in 10 mL of ethanol. To make this solution more dilute for UV-Vis, 0.5 mL of the 3 mM solution were diluted to a volume of 3 mL with ethanol. To prepare 3 mL of a 1 mM solution of $Et_3PAuSpy$, 0.0029 g (0.0068 mmol) were dissolved in ethanol. To make this solution more dilute for UV-Vis, 1 mL of the 1 mM solution was diluted to a volume of 14 mL with ethanol. The concentrations of $Et_3PAuSpy$ and dithiothreitol before titration were 0.1 mM and 0.5 mM respectively. About 2 mL of the 0.5 mM solution of $Et_3PAuSpy$ was transferred to the cuvette and scanned ($Et_3PAuSpy$ in Figure 46). Then, the solution in the cuvette was titrated with the 0.1 mM solution of dithiothreitol by adding one drop at a time and scanning the solution, to create the graph in Figure 45. The range of UV-Vis was 200-500 nm.

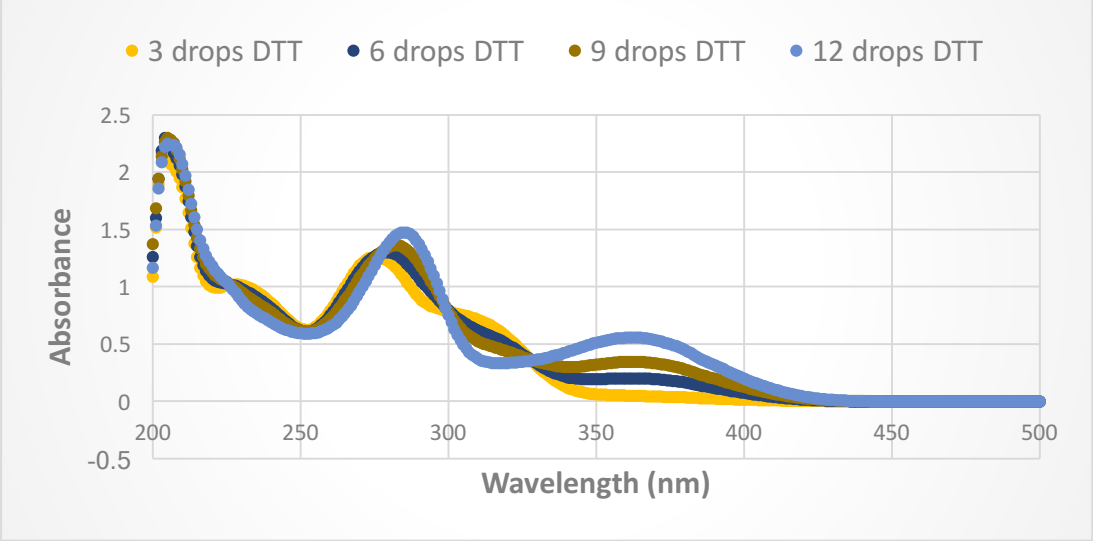

Figure 45: Absorbance plotted as a function of wavelength (nm) of $Et_3PAuSpy$ with DTT, added dropwise

Results and Discussion: Experiment G was carried out to look at the possible reaction between $Et_3PAuSpy$ and DTT. The UV-Vis data was acquired using a titration of $Et_3PAuSpy$ with DTT added dropwise to a solution of $Et_3PAuSpy$ over a period of 30 minutes. Figure 45 shows the absorbance at 3, 6, 9 and 12 drops of DTT added to the cuvette. It can be observed from the graph that $Et_3PAuSpy$ is converted to 2-pyridinethiol in the reaction with DTT with three isosbestic points at approximately 227, 300 and 327 nm. A comparison of the initial spectra of 2-pyridinethiol, DTT and $Et_3PAuSpy$ with the reaction solution of $Et_3PAuSpy$ and DTT is made in Figure 46. It is clear from just comparing the reaction solution with the spectrum of 2-pyridinethiol that it is a conversion of $Et_3PAuSpy$ to 2-pyridinethiol because of the way the peaks are lined up one on top of the other. The ^1H NMR data also supports this conclusion (Figures 47-50). Table 2 (in conjunction with Figure 51) summarizes the ^1H NMR data and gives a thorough comparison of the three spectra. It is clear that $Et_3PAuSpy$ is left over after the reaction is finished, due to the peaks associated with $Et_3PAuSpy$ still being present in the reaction spectrum (Figure 49). However, two new peaks have appeared in the reaction spectrum (Figure 49) that are not attributed to either DTT or $Et_3PAuSpy$. These peaks (c and d as labeled on 2-pyridinethiol) are indications that 2-pyridinethiol has dissociated from the gold complex. 2-pyridinethiol should also theoretically have a peak at 8.62 ppm that integrates for the e proton, but it is not observed on the spectrum of 2-pyridinethiol, which might be a signal to noise ratio problem. There are a couple of impurities in the spectra and several water peaks, but those have been carefully specified in the table. The thiol peaks from 2-pyridinethiol are not observed in addition to the missing DTT OH group peaks, which is common for ^1H NMR spectra. It is proposed from the data that

peak 6 for $Et_3PAuSpy$ is the combination of 2-pyridinethiol's peaks 6 and 7 (the chemical shift due to gold's electron-withdrawing character). It is also proposed that the reaction between $Et_3PAuSpy$ and DTT could form the disulfide pictured in Figure 53. However, this hypothesis can be rejected due to the following two reasons: 1) one of the ^1H NMR peaks for the disulfide (Figure 52) at 8.5 ppm is not observed in the reaction spectrum and 2) while literature values for the UV absorbance for the disulfide show two peaks (238 and 282 nm) (31), the 238 nm peak is not observed in the reaction UV spectrum. Both of these reasons support the conclusion that the disulfide was not a product of the reaction between $Et_3PAuSpy$ and DTT.

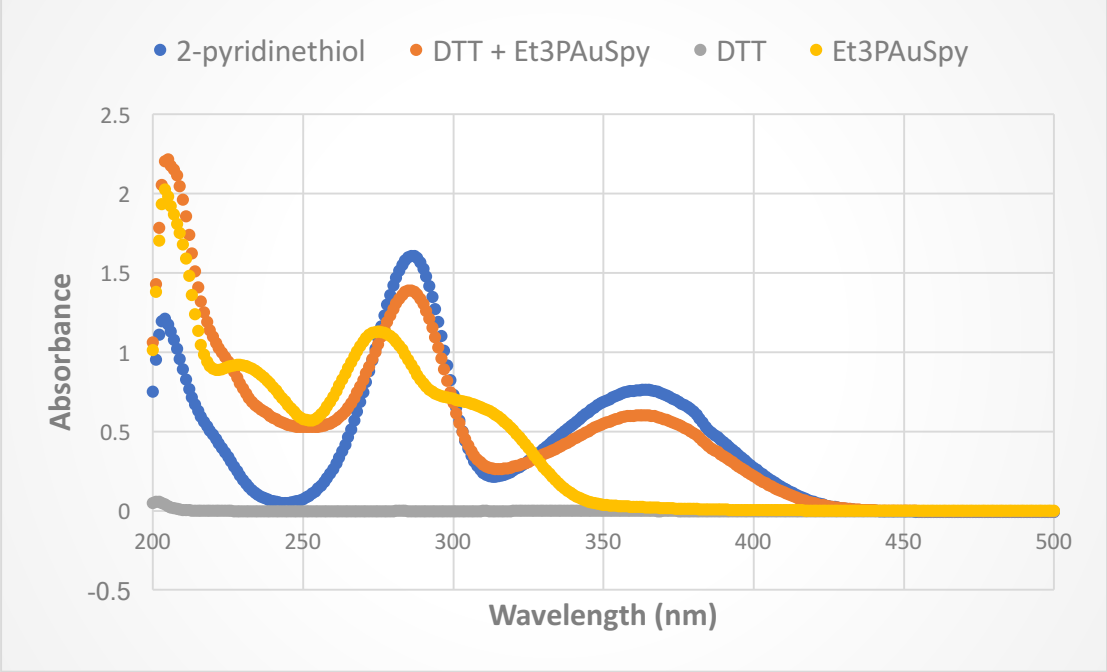

Figure 46: Comparison of 2-pyridinethiol, DTT, $Et_3PAuSpy$ and the reaction of DTT and $Et_3PAuSpy$

^{1}H NMR:

This reaction was also investigated by ^{1}H NMR, by first acquiring a ^{1}H NMR scan of the reactants and then mixing them in a 1:1 volume equivalent and acquiring a scan of the solution in $CDCl_3$ (Figures 47-50).

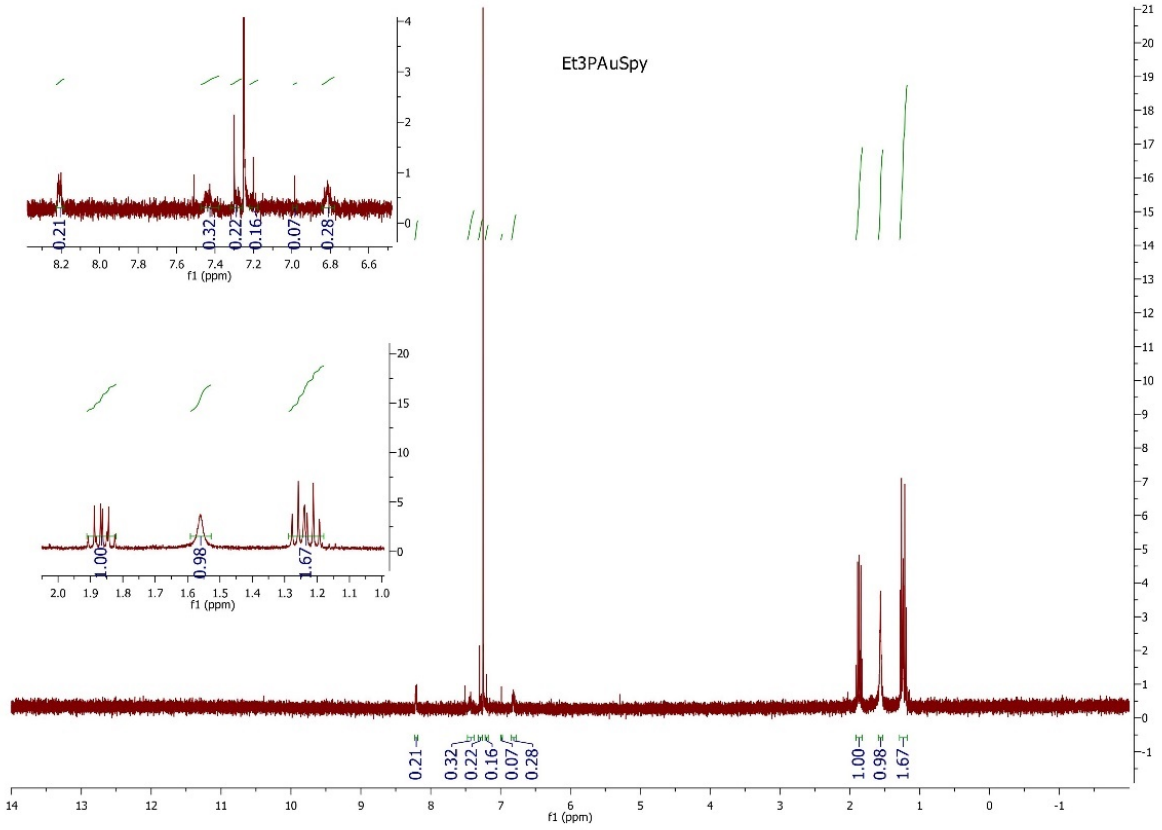

Figure 47: ^{1}H NMR spectrum of $Et_3PAuSpy$ in $CDCl_3$

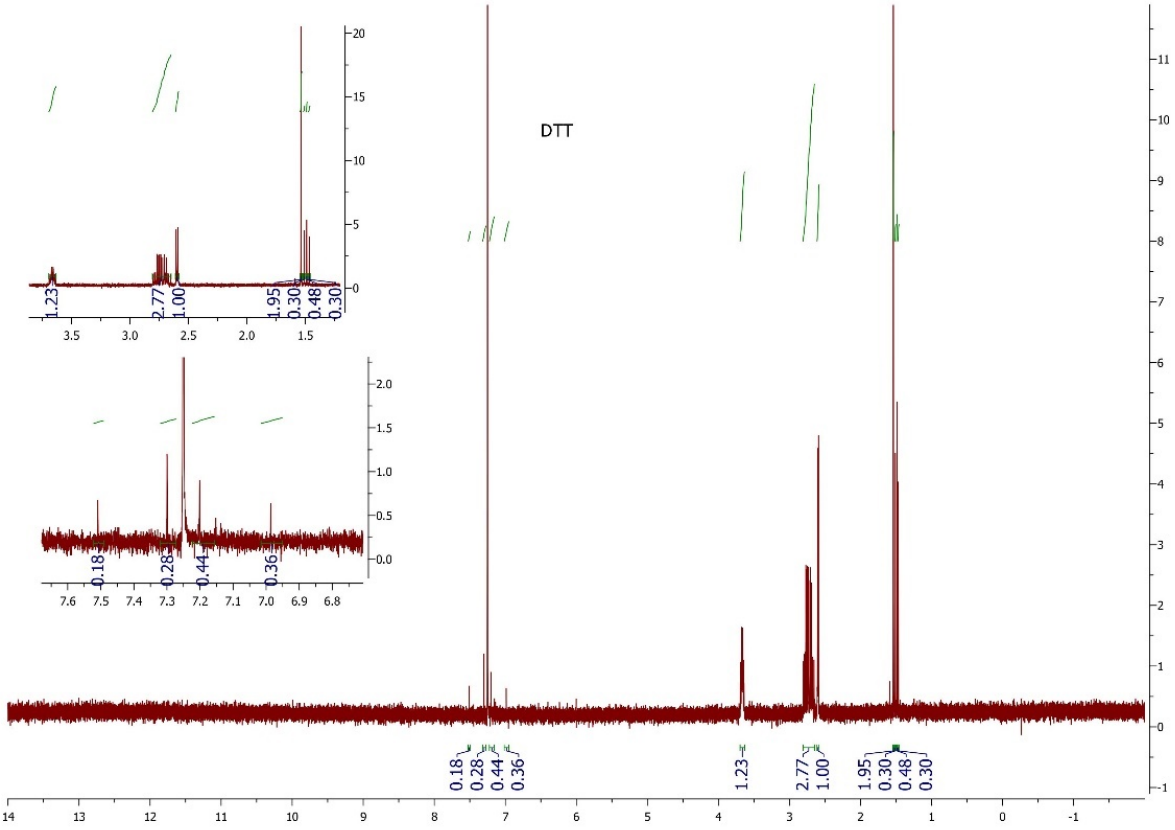

Figure 48: ^{1}H NMR spectrum of DTT in $CDCl_3$

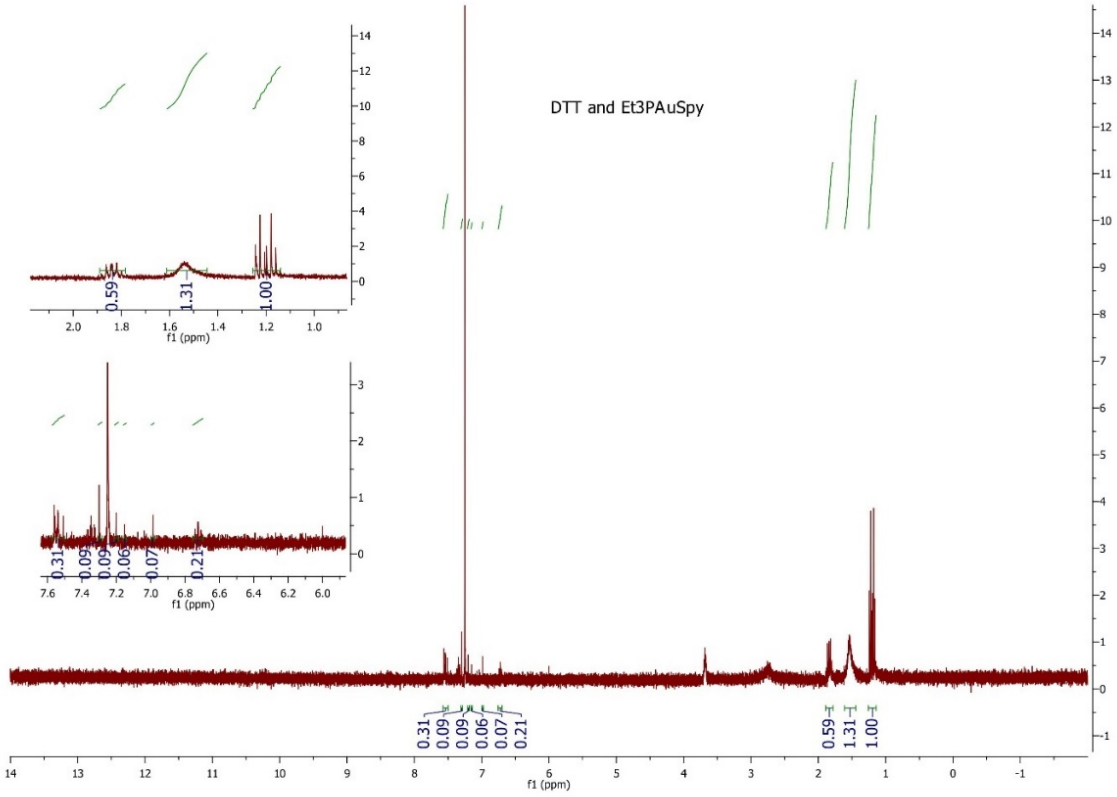

Figure 49: ^{1}H NMR spectrum of the reaction between DTT and $Et_3PAuSpy$ in $CDCl_3$

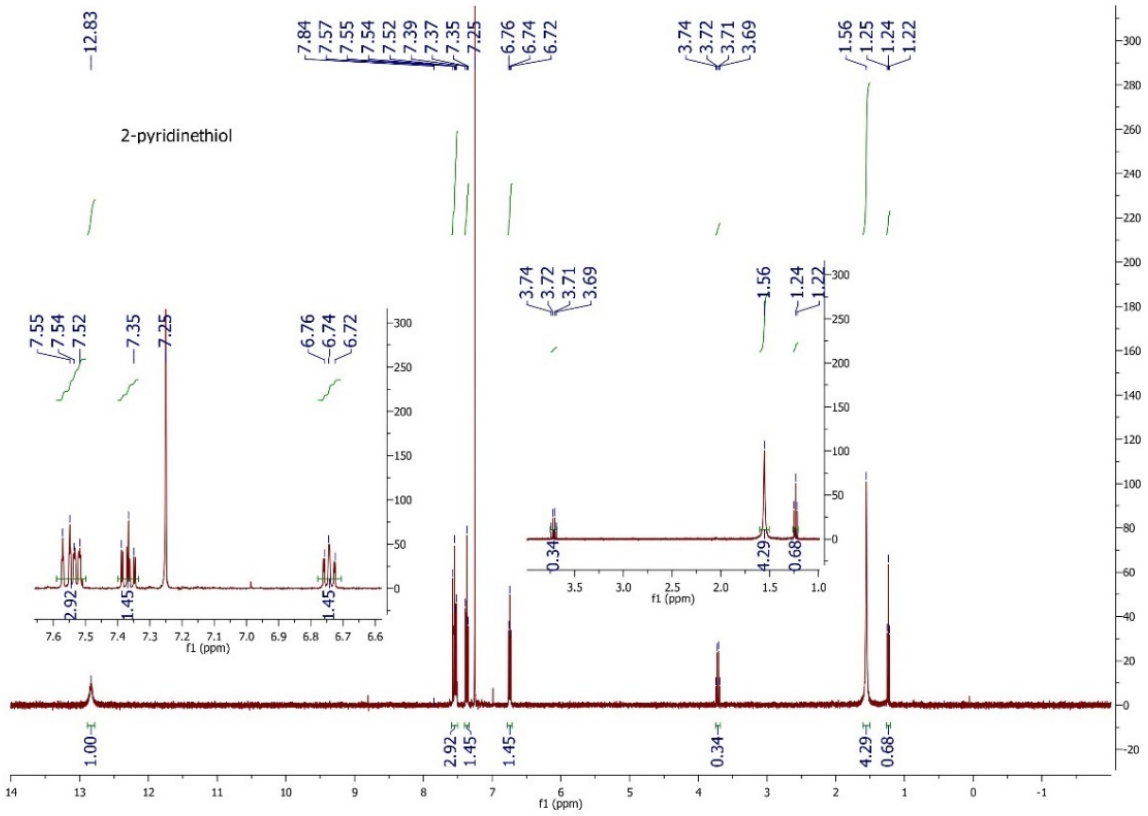

Figure 50: ^{1}H NMR spectrum of 2-pyridinethiol in $CDCl_3$

Table 2: Location of peaks on ^{1}H NMR spectrum and indicated protons

	$Et_3PAuSpy$		***DTT***		***$Et_3PAuSpy$ + DTT***		***2-pyridinethiol***	
Peak	Location (ppm)	Proton Designation	Location (ppm)	Proton Designation	Location (ppm)	Proton Designation	Location (ppm)	Proton Designation
1	1.21	a,c,e	1.5	a,h	1.2	A,c,e ($Et_3PAuSpy$)	1.24	Impurity
2	1.55	Water	2.6-2.75	b,g	1.57	Water (broad peak-not DTT)	1.56	Water
3	1.87	b,d,f	3.7	c,e	1.88	B,d,f ($Et_3PAuSpy$)	3.71	Impurity
4	6.80	g	7.25	$CDCl_3$	2.75	b,g (DTT)	6.74	b
5	7.25	$CDCl_3$	-	-	3.75	c,e (DTT)	7.25	$CDCl_3$
6	7.45	i,h	-	-	6.8	g ($Et_3PAuSpy$)	7.37	c
7	8.22	j	-	-	7.0	Impurity	7.56	d
8	-	-	-	-	7.2	Impurity	12.93	Impurity (OH)
9	-	-	-	-	7.25	$CDCl_3$	-	-
10	-	-	-	-	7.3	Impurity	-	-
11	-	-	-	-	7.37	c (2-pyr)	-	-
12	-	-	-	-	7.55	d (2-pyr)	-	-
13	-	-	-	-	8.2	j ($Et_3PAuSpy$)	-	-

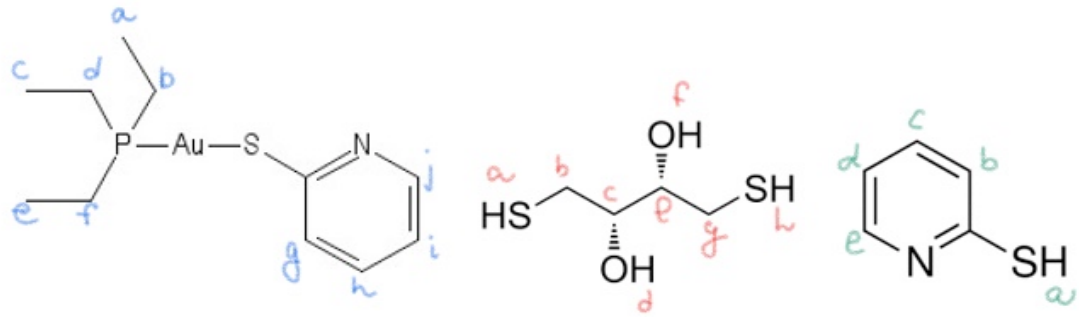

Figure 51: Proton labeling from left to right: $Et_3PAuSpy$, DTT and 2-pyridinethiol

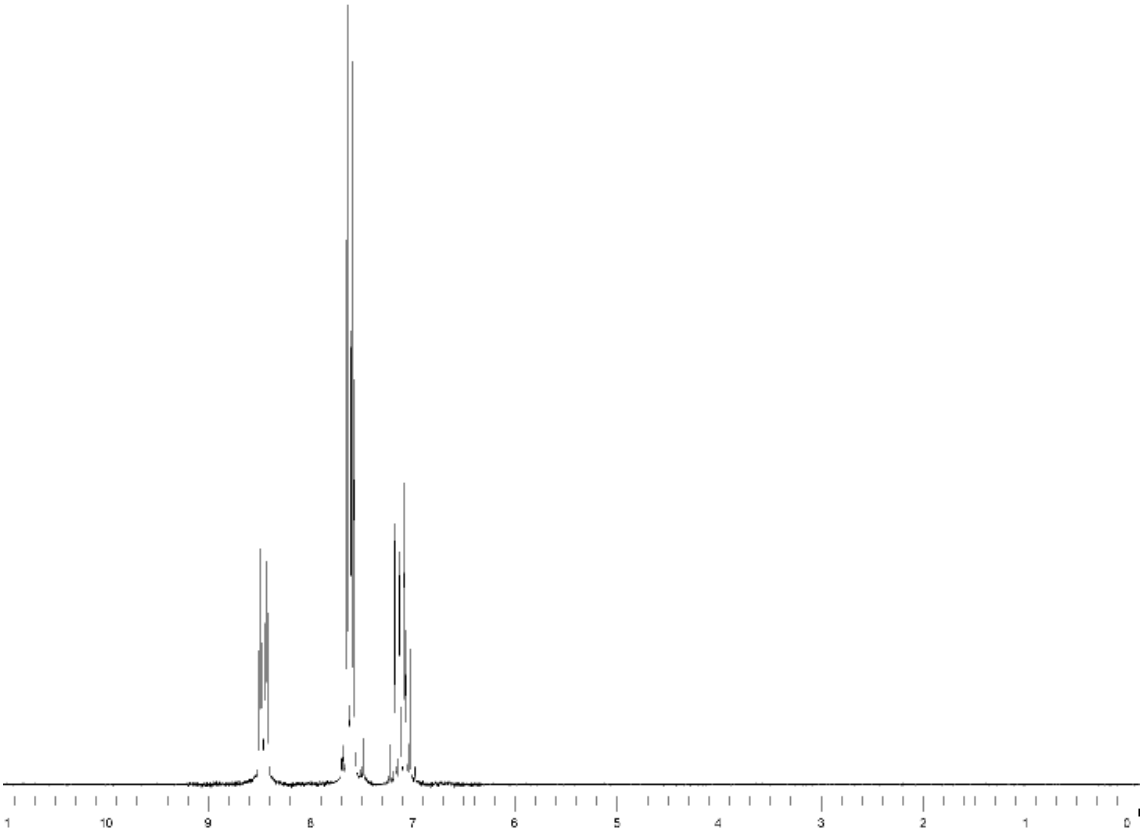

Figure 52: ^{1}H NMR spectrum of 2-pyridinethiol disulfide (SciFinder)

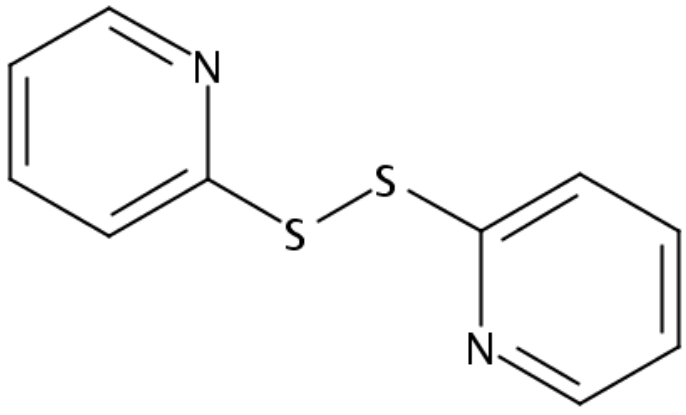

Figure 53: Possible 2-pyridinethiol disulfide

Oxidized DTT

DTT is unstable in its reduced form and its oxidation can be further catalyzed by metal ions[41]. A study in 2013 showed that the redox potential of the reaction changed by 3-5% during the 2.5 hrs needed for the reactions investigated[41]. Even though it has often been assumed that under anaerobic conditions and in the presence of a chelating agent such as EDTA the reaction should maintain a constant redox potential, the 2013 study proved this assumption false[41]. In general, this should not be an issue at small enough concentrations of DTT; however, the possibility of DTT oxidizing while sitting in solution for some time was tested by UV-Vis. The solution of DTT used for the titration was scanned initially and after 30 minutes. Unlike reduced DTT, which is not UV active, oxidized DTT is UV active with an absorbance peak at 283 nm (Figure 54)[14]. The scan of the DTT solution after sitting for 30 minutes showed no absorbance peak, therefore suggesting that DTT does not oxidize while sitting in solution for the amount of time required to do the titration of $Et_3PAuSpy$ with DTT (Figure 55).

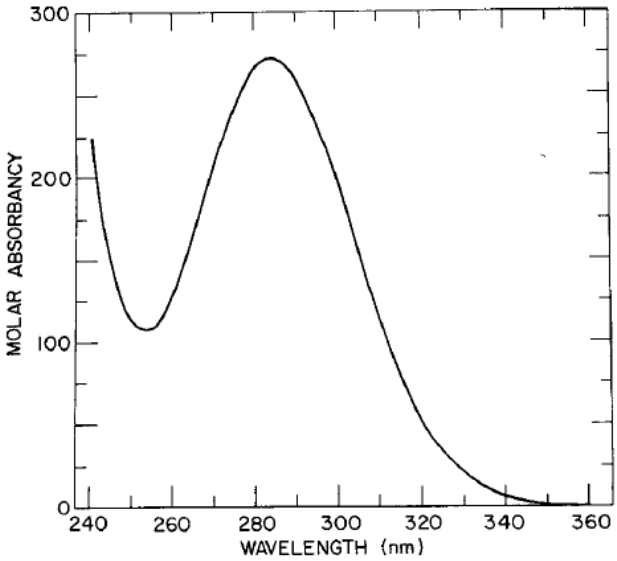

Figure 54: Molar absorbance of oxidized DTT as a function of wavelength. Solvent is 0.05 M phosphate buffer, pH 8[14].

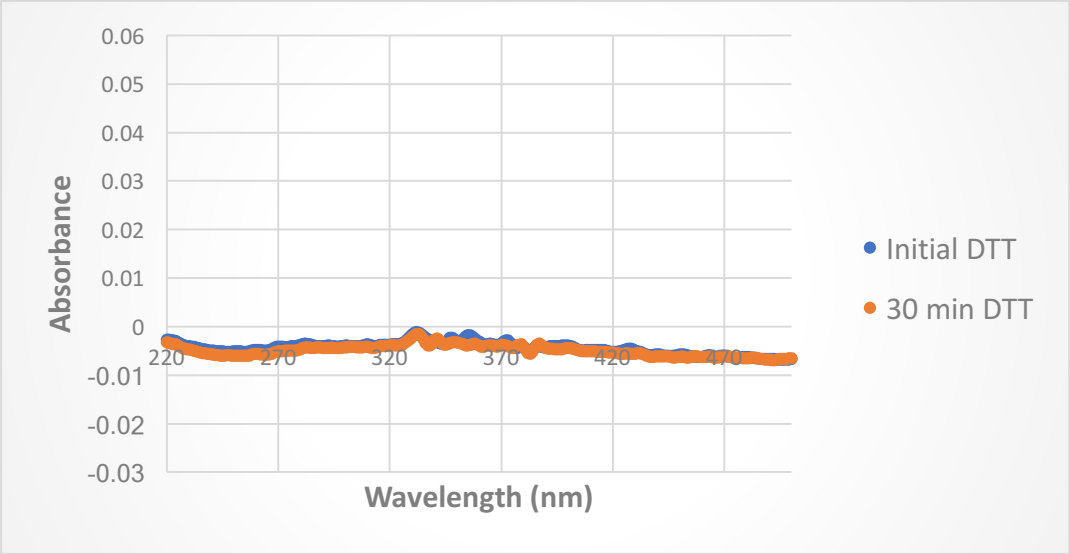

Figure 55: UV-Vis scan of the DTT solution right after it was made and after it has been sitting uncovered for 30 minutes (the time interval it took for the titration), showing no oxidizing activity, as DTT_{red} is not UV-active, while DTT_{ox} is UV-active (peak at 282 nm).

Experiment H (Et3PAuCl and insulin)

Methods: To prepare 3.7 mL of a 5.0 mM $Et_3PAuSpy$ solution, 0.0065 g (0.0185 mmol) were dissolved in phosphate buffer. The solution was stirred until all of the solid was dissolved in the solution. Insulin stock solution 2 was warmed to room temperature. The UV-Vis was autozeroed on phosphate buffer, not air. To make the cuvette solution, 1 mL of insulin stock solution 2 was added to the cuvette, followed by 1.86 mL of phosphate buffer and 160.0 µL of Et_3PAuCl solution. The UV-Vis was set up to scan the cuvette every 3 minutes (including the 25 sec it takes to actually perform a scan) in the wavelength range of 300-800 nm. The total number of scans was 242 (approx. 12 hrs). The absorbance at 650 nm as a function of time in minutes was plotted in Figure 56.

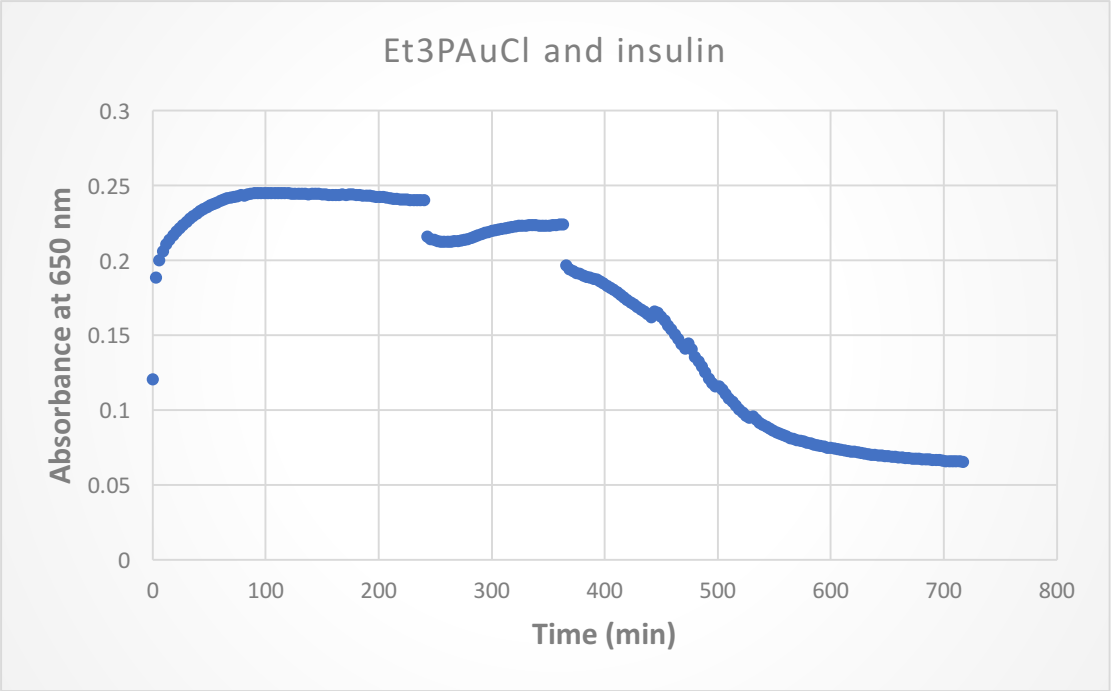

Figure 56: Absorbance at 650 nm plotted as a function of time of the reaction between Et_3PAuCl and insulin

Results and Discussion: Experiment H was carried out to see how Et_3PAuCl would react with insulin. According to the UV spectrum above, Et_3PAuCl does react with insulin, but the four-centered metallacycle intermediate mechanism proposed for the reaction between $Et_3PAuSpy$ and insulin does not seem likely in this case, due to the nature of Et_3PAuCl, which usually undergoes a ligand-substitution. However, the thiol-containing amino acid cysteine was found to react with bromo(triethylphosphine)gold in aqueous solution[42]. The product, 2-amino-2-carboxyethylthio(triethylphosphine)gold (Figure 57) was unstable and its aqueous solution slowly deposited an amorphous precipitate of aurous cysteinate[42]. A freshly made solution of the product was acidified with hydrochloric acid to give cysteine and chloro(triethylphosphine)gold[42]. This seems to suggest that Et_3PAuCl can react with the cysteine residues of insulin in the same manner,

that is if the cysteines were free and were not part of disulfide bonds. It is possible that Et_3PAuCl may be interacting with nearby amino acids that have donor atoms, such as histidine. However, a mechanism for this reaction cannot be gleaned at this point in the research.

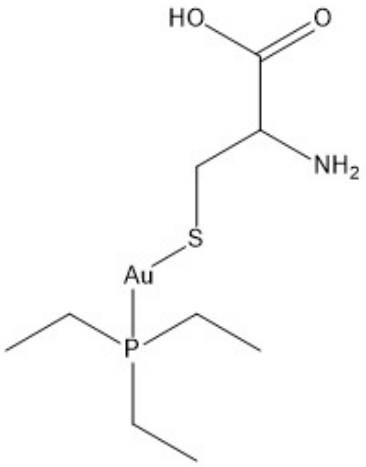

Figure 57: Structure of 2-amino-2-carboxyethylthio(triethylphosphine)gold

Experiment I (Et3PAuCl and DTT)

UV-Vis:

Methods: To prepare 10 mL of 3 mM solution of dithiothreitol, 0.0046 g (0.0298 mmol) were dissolved in 10 mL of ethanol. To make this solution more dilute for UV-Vis, 0.5 mL of the 3 mM solution were diluted to a volume of 3 mL with ethanol. To prepare 10 mL of a 1 mM solution of Et_3PAuCl, 0.0035 g (0.0099 mmol) were dissolved in ethanol. To make this solution more dilute for UV-Vis, 1 mL of the 1 mM solution was diluted to a volume of 15 mL with ethanol. The final concentrations of Et_3PAuCl and dithiothreitol were 0.1 mM and 0.5 mM respectively. About 2 mL of the 0.1 mM solution of Et_3PAuCl was transferred to the cuvette and scanned, showing no peak, which was expected as Et_3PAuCl is not UV active. Then, the solution in the cuvette was titrated with the 0.5 mM solution of dithiothreitol by adding one drop at a time and scanning the solution. The range of UV-Vis was 200-500 nm. There were no observable peaks as more DTT was added dropwise, suggesting that DTT does not react with Et_3PAuCl.

^{1}H NMR:

To confirm this hypothesis, the reaction was also investigated using ^{1}H NMR, by first acquiring a ^{1}H NMR scan of the reactants and then mixing them in a 1:1 volume equivalent and acquiring a scan of the solution in $CDCl_3$ (Figures 59-61). Table 3 in conjunction with Figure 62 summarize the ^{1}H NMR data and give a comparison between reactants and the reaction solution.

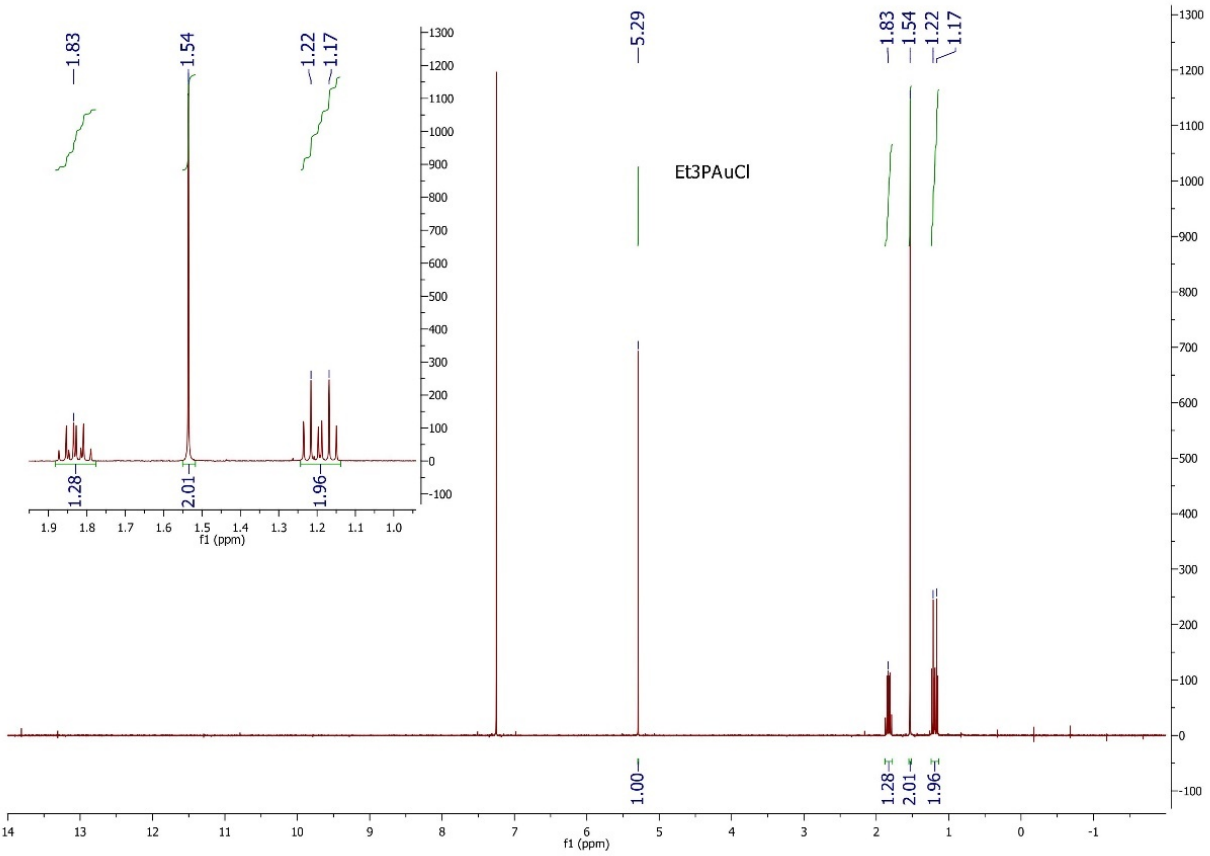

Figure 59: ^{1}H NMR spectrum of Et_3PAuCl in $CDCl_3$

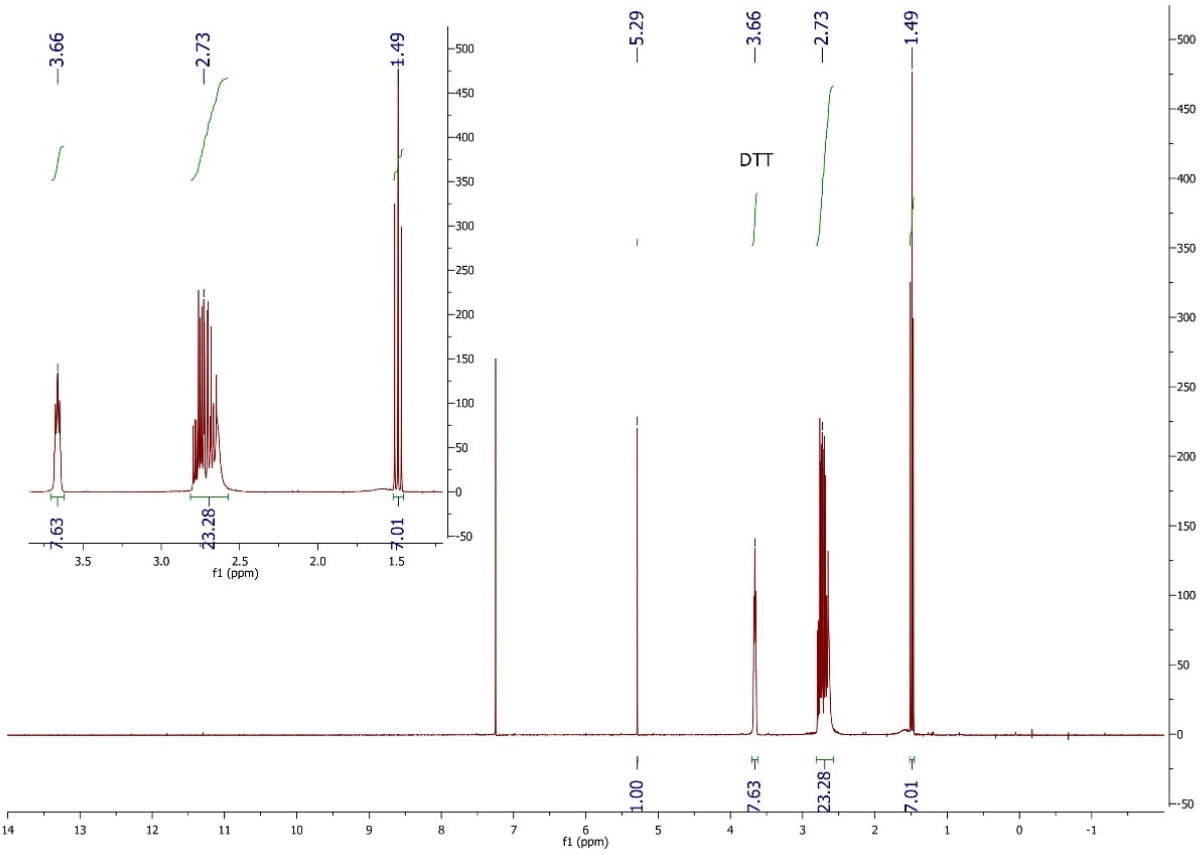

Figure 60: ^{1}H NMR spectrum of DTT in $CDCl_3$

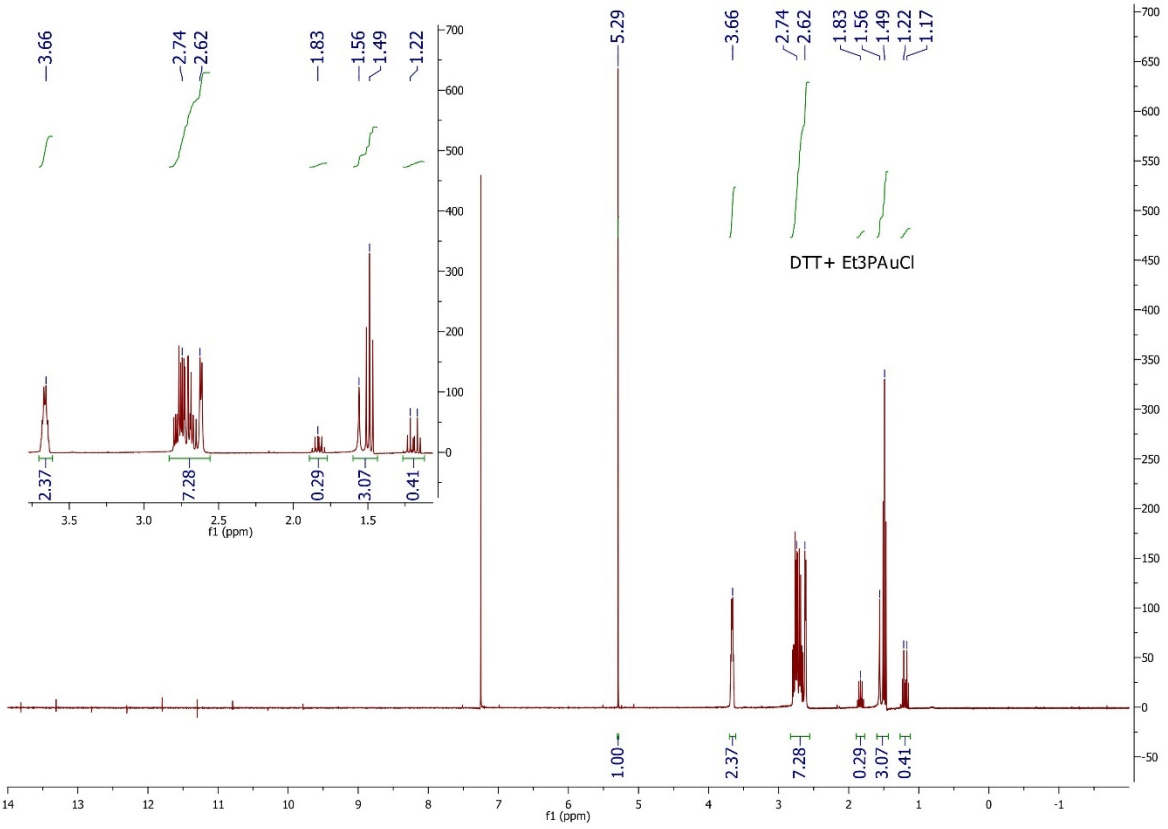

Figure 61: ^{1}H NMR spectrum of the reaction between Et_3PAuCl and DTT in $CDCl_3$

Table 3: Location of peaks on ^{1}H NMR spectrum and indicated protons

	Et_3PAuCl		***DTT***		***Et_3PAuCl + DTT***	
Peak	Location (ppm)	Proton Designation	Location (ppm)	Proton Designation	Location (ppm)	Proton Designation
1	1.19	a,d,f	1.49	a,h	1.19	a,d,f (Et_3PAuCl)
2	1.54	Water	2.73	b,g	1.49-1.56	a,h (DTT) and water
3	1.83	b,c,e	3.66	c,e	1.83	b,c,e (Et_3PAuCl)
4	5.29	Impurity	5.29	Impurity	2.62-2.74	b,g (DTT)
5	7.25	$CDCl_3$	7.25	$CDCl_3$	3.66	c,e (DTT)
6	-	-	-	-	5.29	Impurity
7	-	-	-	-	7.25	$CDCl_3$

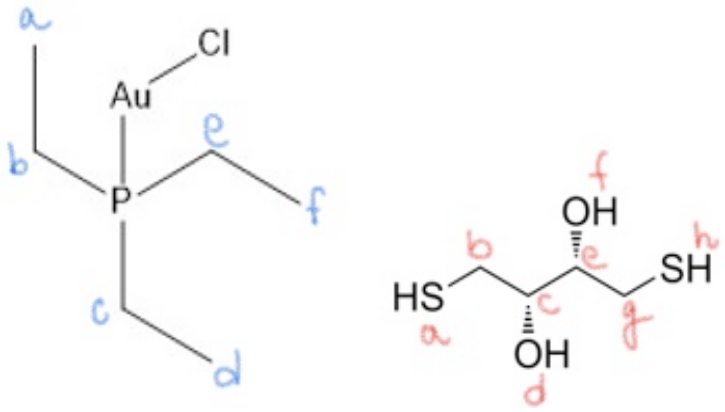

Figure 62: Proton labeling from left to right: Et_3PAuCl and DTT

Results and Discussion: Experiment I was carried out to compare the reaction between DTT and Et_3PAuCl (Experiment H) and DTT and $Et_3PAuSpy$ (Experiment I). Et_3PAuCl and reduced DTT are not UV-Vis active, and therefore show no absorbance. The goal of the experiment was to observe using UV-Vis the possible appearance of a peak to indicate the formation of a product. No such peak appeared. The ^1H NMR data showed that the reaction solution of DTT and Et_3PAuCl showed all of the peaks that DTT and Et_3PAuCl showed separately and no chemical shifts were observed. The peak at 5.29 ppm was a methylene chloride peak that showed reagent bottle contamination. It seems plausible from UV and ^1H NMR data that Et_3PAuCl and DTT do not react. Since Et_3PAuCl and DTT would have reacted through a simple ligand substitution, it seems like $Et_3PAuSpy$ and DTT do not go through a ligand substitution mechanism.

Furthermore, it is possible that the DTT forms a complex with Et_3PAuCl, whereby it links two of the molecules together (Figure 63)[43]. However, since there is no indication of chemical shifts, there is no reason to think the dimer was formed.

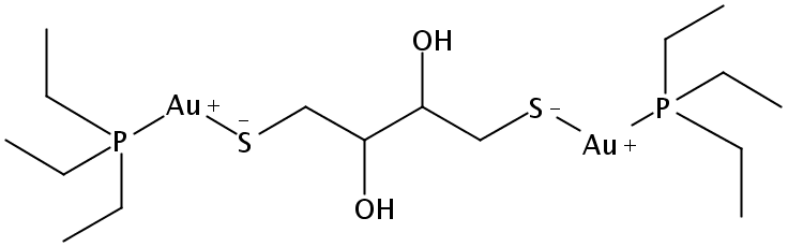

Figure 63: Possible product of the reaction between Et_3PAuCl and DTT

It is useful to mention that dithioerythritol (DTE), an isomer of DTT was successfully reacted with Et_3PAuCl in a 50/50 mixture of ethanol and water under vigorous stirring to form a white precipitate in one study[43]. An indicator that the reaction occurred was the

sudden acidification of the solution[43]. It is possible that Et_3PAuCl may react with DTT under likewise conditions.

DISCUSSION

Approximately 20% of all human proteins are predicted to contain disulfide bonds[4]. With this abundance in the human organism, it is important to study thiol-disulfide exchange reactions using biological models to gain insight into how disease-specific drugs may be interacting with proteins in the body. By looking at how gold thiolates interact with protein disulfides using insulin as a model protein disulfide, this experiment was able to look at how gold thiolates might be interacting with biological disulfides in a gold thiolate-disulfide exchange reaction.

The study was started by replicating two experiments performed by the Lees research group, namely the reaction between 4-mercaptobenzoic acid, DTT and insulin compared to the reaction between DTT and insulin. The method of data collection used was UV-Vis spectroscopy, but it was used to observe light scatter at 650 nm, instead of the usual absorbance method. When the disulfide bonds in insulin are reduced, the two chains of insulin break apart, forming a colloidal suspension. This suspension scatters light at 650 nm, which provides a curve that shows an initial lag time (which can be attributed to the particles not having yet reached a critical concentration at which they start aggregation), followed by a steady increase in light scatter (aggregation), which is directly proportional to the extent to which the insulin disulfide bonds have been broken. After reaching a certain maximum, the particles become too dense to stay in the colloidal suspension and sink to the bottom, which is why the rate of particle formation decreases after reaching a maximum. The relative rate that was acquired during this study (approximately 1.7) was

close to the value reported by Lees of 1.6, showing that 4-mercaptobenzoic acid catalyzes the reaction between DTT and insulin. This was a good starting point for the study, and the results are depicted in Experiments A and B. The next step of the study was to see if 4-mercaptobenzoic acid would break the disulfide bonds in insulin without the assistance of DTT. Experiment C showed no reaction as monitored by UV-Vis over 24 hours. This suggested that either 4-mercaptobenzoic acid does not react with insulin, or that the lag time of the reaction is very long and is beyond the scope of the 24 hours that was dedicated to the reaction.

The next step of the study was to try a gold thiolate in the reaction between DTT and insulin to see if the gold compound would have the same effect as the aromatic thiol used previously (4-mercaptobenzoic acid). However, when synthesized, $Et_3PAuSba$ was not soluble in phosphate buffer, which was the solvent system that was being used for the experiments. Thus, it became necessary to change the thiol that was being investigated, so that once the gold thiolate that had the thiol moiety attached to it was synthesized, it would be soluble in phosphate buffer. This would ensure that all reactants were fully soluble in the solvent and any precipitation observed would be caused by the breaking of the disulfide bonds in insulin and the formation of the colloidal suspension of α and β chain particles. The thiol that was picked as a replacement was 2-mercaptopyridine, which was available in lab, and it was known that $Et_3PAuSpy$ was soluble in phosphate buffer. Experiment D was conducted to observe the reaction between 2-mercaptopyridine, DTT and insulin. A comparison was made between 2-mercaptopyridine's and 4-mercaptobenzoic acid's effect on the rate of the reaction

between DTT and insulin. The graphs of these two experiments were nearly completely overlapping, suggesting similar results for effect on the rate of the reaction between DTT and insulin.

The next step of the study was to see what effect the gold thiolate would have on the rate of the reaction between DTT and insulin. This was the purpose of Experiment E. The graph obtained showed an initial increase, followed by a drastic decrease in slope, yet still increasing for some time and then another drastic increase in slope. This kind of graph was a surprise, because it indicated the possibility that there could be several mechanisms at work when combining $Et_3PAuSpy$, DTT and insulin. As was found by Experiments E and F, which looked at the reaction between $Et_3PAuSpy$ and insulin and the reaction between $Et_3PAuSpy$ and DTT respectively, these reactions were occurring by different mechanisms. The reaction between $Et_3PAuSpy$ and insulin produced the familiar colloidal suspension of α and β chain particles. The reaction between $Et_3PAuSpy$ and DTT was shown to produce 2-mercaptopyridine by both UV-Vis and ^1H NMR. This suggests that the prediction about Experiment E ($Et_3PAuSpy$, DTT and insulin), namely that there might be several competing mechanisms that give the different shape of the graph, might have merit.

The next step in the study was to look at how Et_3PAuCl would react with insulin. This was the purpose of Experiment H. The graph of the experiment showed the formation of a colloidal suspension, but several breaks in the graph suggest either instrument malfunction or possibly interesting particle formation dynamics. Since the experiment

was not replicated, it is hard to say which of those is more plausible. The reproducibility aspect is addressed further below. The observation that Et_3PAuCl reacts with insulin makes analysis harder, since Et_3PAuCl would not break the disulfide bonds by thiol-disulfide exchange and would instead want to participate in a ligand-substitution reaction. This makes the results of this experiment interesting, because it suggests that Et_3PAuCl is interacting with other amino acids in insulin, possibly such donor atom-containing amino acids as histidine. Lastly, Experiment I was conducted to look at the possible reaction between Et_3PAuCl and DTT. Neither UV-Vis nor ^1H NMR showed that a reaction was occurring. It is possible that the conditions in which the reaction was conducted were not optimal. DTT has to be deprotonated under basic conditions to react, and the UV-Vis reaction was conducted in methanol, which is technically an acid and a base at the same time. The ^1H NMR reaction was carried out in deuterated chloroform, which is acidic because of the induction affects from the chloride groups. It is possible that DTT did not have a chance to be deprotonated and thus was not able to react.

CONCLUSION

As far as specific conclusions that could be made from this study, they are as follows: 1) 4-mercaptobenzoic acid and 2-mercaptopyridine catalyze the reaction between DTT and insulin, likely by the same mechanism, as supported by the Lees research group findings and UV-Vis data. 2) $Et_3PAuSpy$ seems to catalyze the reaction between DTT and insulin more so than the aromatic thiols, although it was also seen reacting with insulin directly, with no DTT present. $Et_3PAuSpy$ was also shown to react with DTT to produce 2-pyridinethiol. As of now, it is unclear as to how the three of them react in solution. It is predicted that once all three are combined in solution, there are several competing mechanisms that occur together. 3) Et_3PAuCl and insulin were shown to react. It is predicted that Et_3PAuCl reacts with donor atom-containing amino acids in insulin such as histidine, which could cause precipitation of insulin molecules.

FUTURE WORK

An important point to consider is that while these studies are concerned with observing the reaction between insulin and a variety of thiols and thiolates, the reaction happens in a phosphate buffer system. One of the reasons this research is important is to facilitate the purification and correct refolding of disulfide-containing proteins from recombinant inclusion bodies (insoluble protein aggregates)[44]. However, the folding of inclusion bodies of disulfide-containing proteins is typically performed in the presence of a denaturant such as guanidine hydrochloride or urea, while this research was not conducted with a denaturant present[44]. It is, however, important to point out that studies on the reaction between RNase A and small ortho- and meta-substituted aromatic thiols *in the presence of denaturants* provided 100% recovery of active protein without significant alteration of protein-folding rates[44]. It would be interesting to see whether gold thiolates would have the same effect.

Additionally, the experiments performed in this study have not been replicated to the extent as to be able to talk about error and reproducibility. The first two experiments (Experiment A: 4-mercaptobenzoic acid, DTT and insulin; Experiment B: DTT and insulin) have been done by the Lees research group, and their relative rate of 1.6 showed that 4-mercaptobenzoic acid catalyzed the breaking of the insulin disulfide bonds, therefore increasing the rate of the formation of the colloidal suspension. The results of Experiments A and B give an approximate relative rate of 1.7, which is close to the Lees relative rate of 1.6. This suggests that Experiments A and B reproduced the results acquired by the Lees research group. However, to be certain that the conclusions of this

study are valid, each experiment would need to be replicated at least 3-4 times to be able to calculate the mean rate and the standard deviation from the mean to be able to discuss precision and reproducibility. Especially experiments that had unexpected artifacts or outcomes (such as Experiment H, Figure 56) would need to be replicated to see whether those artifacts (such as breaks in the graph) are due to improper instrumentation function or are indications of complicated mechanisms that would warrant further study of the reaction. The reaction of Et_3PAuCl with DTT was also most likely conducted under improper conditions, as DTT has to be deprotonated under basic conditions, while the two solvents used for the UV-Vis and ^1H NMR experiments were methanol and deuterated chloroform respectively. This could provide nonideal conditions for this reaction and it might thus be possible to react Et_3PAuCl with DTT under different conditions.

The factors that have been shown to be important advantages for protein folding catalysts as indicated by Lees are as follows:

1) Low thiol pKa (strongly acidic thiol, weakly basic thiolate-close to physiological pH), a pKa of approximately 1 unit less than the pH of the solution has been found to be optimal for protein folding, with increased thiolate reactivity[4]
2) Low reduction potential (allows the catalyst to exist as a nearly 50:50 mixture of thiol and disulfide for efficient protein folding)[4]
3) Dithiol over a monothiol (dithiols discourage forming long-lived mixed disulfides between the folding catalyst and the protein of interest)

4) Aromatic thiols increase the rate of folding by at least three times as opposed to aliphatic thiols

In developing more efficient protein folding catalysts it is important to keep these factors in mind. In the case of gold thiolates, a possible development of an aromatic gold dithiol with a low pKa might be advantageous for further studies in regard to the redox buffer.

A look at the different variables that can be changed in the study is also warranted. Studies can be designed that change variables that were kept constant during this study but might shed some light on the results. For example, it might be interesting to look at the way the rate of formation of the colloidal suspension (the rate of disulfide bond breakage) changes when the reaction is stirred, when the temperature is changed or when the pH is changed (keeping in mind that insulin is only soluble in a buffer of pH 6-8). These studies could account for such things as diffusion (since the reactions were not stirred in this experiment) and the mean aggregation rate could be acquired instead of the initial rate.

Insulin is used as a model protein because it has three disulfide bonds and is readily commercially available; however, the study can be opened to other proteins containing disulfides. Other methods of data collection might also prove more optimal than light scatter, such as Particle Size Distribution, which could shed some light on such reactions as $Et_3PAuSpy$, DTT and insulin, which is predicted to react in several different competing mechanisms ($Et_3PAuSpy$ reacts both with DTT and insulin, and DTT reacts with insulin as well, all react by different mechanisms). Other useful techniques could be

HPLC (to look at the formation of oxidized DTT) or mass spectrometry, which would further the studies previously discussed in the Introduction, and in which Me_3PAu^+ proved a very promising compound for the breaking of disulfide bonds in gas-phase reactions.

REFERENCES

1. DeCollo, Todd V.; Lees, Watson J. "Effects of aromatic thiols on thiol-disulfide interchange reactions that occur during protein folding" *J. Org. Chem*., **2001**, *66*, 4244-4249

2. De Levie, R. "Redox Buffer Strength" *Journal of Chemical Education*, **1999**, *76 (4),* 574-577.

3. Owen J.B., Butterfield D.A. (2010) Measurement of Oxidized/Reduced Glutathione Ratio. In: Bross P., Gregersen N. (eds) Protein Misfolding and Cellular Stress in Disease and Aging. Methods in Molecular Biology (Methods and Protocols), vol 648. Humana Press, Totowa, NJ

4. Lees, W.J.; "Small-molecule catalysts of oxidative protein folding" *Current Opinion in Chemical Biology*, **2008**, *12*, 740-745.

5. Patel, A.S.; Lees, W.J.; "Oxidative folding of lysozyme with aromatic dithiols, and aliphatic and aromatic monothiols" *Bioorganic & Medicinal Chemistry*, **2012**, *20*, 1020-1028.

6. Berner-Price, S.J.; Filipovska, A. "Gold compounds as therapeutic agents for human diseases" *Metallonomics*, **2011**, *3*, 863-873

7. Berners-Price, S.J.; "Gold-based therapeutic agents: a new perspective" *Bioinorganic Medicinal Chemistry*, **2011**, 197-216

8. Mohamed, A.A.; Abdou, H.E.; Chen, J.; Bruce, A.E.; Bruce, M.R.M.; "Perspectives in inorganic and bioinorganic gold sulfur chemistry" *Comments on Inorganic Chemistry*, **2002**, *23*, 321-334

9. Ashraf, W.; Isab, A.; "^{31}P NMR studies of redox reactions of Bis(Trialkylphosphine) gold(I) bromide (alkyl=methyl, ethyl) with disulfide and diselenide" *J. Coord. Chem.*, **2004**, *57(4)*, 337-346.

10. Deponte, M.; Urig, S.; Arscott, D.; Fritz-Wolf, K.; Reau, R.; Herold-Mende, C.; Koncarevic, S.; Meyer, M.; Davioud-Charvet, E.; Ballou, D.P.; Williams, C.H.; Becker, K.; "Mechanistic studies on a novel, highly potents gold-phosphole inhibitor of human glutathione reductase" *The Journal of Biological Chemistry***, 2005**, *280(21)*, 20628-20637.

11. Mirabelli, C.K.; Johnson, R.K.; Hill, D.T.; Faucette, L.F.; Girard, G.R.; Kuo, G.Y.; Sung, C. M.; Crooke, S.T.; "Correlation of the in vitro cytotoxic and in vivo

antitumor activities of gold(I) coordination complexes" *J. Med. Chem.*, **1986**, *29*, 218-223

12. Gough, J.D.; Lees, W.J.; "Increased catalytic activity of protein disulfide isomerase using aromatic thiol based redox buffers" *Bioorganic & Medicinal Chemistry Letters*, **2005**, *15*, 777-781.

13. Gurbhele-Tupkar, M.C.; Lissette, R.P.; Silva, Y.; Lees, W.J.; "Rate enhancement of the oxidative folding of lysozyme by the use of aromatic thiol containing redox buffers" *Bioorganic & Medicinal Chemistry*, **2008**, *16*, 2579-2590.

14. Iyer, K.S.; Klee, W.; "Direct spectrophotometric measurement of the rate of reduction of disulfide bonds" *The Journal of Biological Chemistry*, **1973**, *248(2)*, 707-710.

15. Wilden, P.A.; Boyle, T.R.; Swanson, M.L.; Sweet, L.J.; Pessin, J.E.; "Alteration of intramolecular disulfides in insulin receptor/kinase by insulin and dithiothreitol: insulin potentiates the apparent dithiothreitol-dependent subunit reduction of insulin receptor" *Biochemistry*, **1986**, *25*, 4381-4388.

16. Fukada, H.; Takahashi, K.; "Calorimetric study of the reduction of the disulfide bonds in insulin" *Journal of Biochemistry*, **1980**, *87(4)*, 1111-1117.

17. Fukada, H.; Takahashi, K.; "Enthalpy and heat capacity changes for the reduction of insulin" *Biochemistry*, **1982**, *21*, 1570-1574.

18. Zhang, Na.; Marahatta, R.; Lees, W.J.; "Folding analysis of bovine pancreatic trypsin inhibitor (BPTI) with aromatic thiols and disulfides in vitro" Abstracts of Papers, 255th ACS National Meeting & Exposition, New Orleans, LA, United States, March 18-22, 2018.

19. Weiss, M.; "Proinsulin and the genetics of diabetes mellitus" *Journal of Biological Chemistry*, **2009**, *284(29)*, 19159-19163.

20. Fang, X.; Yang, T.; Wang, L.; Yu, J.; Wei, X.; Zhou, Y.; Wang, C.; Liang, W.; "Nano-cage mediated refolding of insulin by PEG-PE miscelle" *Biomaterials*, **2016**, *77*, 139-148.

21. Lindley, H.; "The reduction of the disulfide bonds of insulin" *J. Am. Chem. Soc*., **1955**, *77(18)*, 4927-4929.

22. Holmgren, A.; "Thioredoxin catalyzes the reduction of insulin disulfides by dithiothreitol and dihydrolipoamide" *The Journal of Biological Chemistry*, **1979**, *254, 19*, 9627-9632

23. Chang, S.; Choi, K.; Jang, S.; Shin, H.; "Role of disulfide bonds in the structure and activity of human insulin" *Mol. Cells.*, **2003**, *16(3)*, 323-330.

24. Sohn, C.H.; Gao, J.; Thomas, D.A.; Kim, T.; Goddard, W.A.; Beauchamp, J.L.; "Mechanisms and energetics of free radical initiated disulfide bond cleavage in model peptides and insulin by mass spectrometry" *Chem. Sci.*, **2015**, *6*, 4550-4560.

25. Groskreutz, D.J.; Sliwkowski, M.X.; Groman, C.; "Genetically engineered proinsulin constitutively processed and secreted as mature, active insulin" *The Journal of Biological Chemistry*, **1994**, *269(8)*, 6241-6245.

26. "Insulin: An early structure with sweet success" Protein Data Bank Europe, pdbe.org

27. Mentinova, M.; McLuckey, S.; "Cleavage of multiple disulfide bonds in insulin via gold cationization and collision-induced dissociation" *International Journal of Mass Spectrometry*, **2011**, *308*, 133-136

28. Markus, G.; "Electrolytic reduction of the disulfide bonds of insulin" *The Journal of Biological Chemistry*, **1964**, *239(12)*, 4163-4170.

29. "Ramachandran plots. Amino acid configuration in proteins" Chemistry 351, www.greely.org/~hod/papers/Unsorted/Ramachandran.doc.pdf

30. Komori, K.; Nakayama, H.; Nakagawa, S.; "Effects of dithiothreitol (DTT) on insulin binding to the membranes of rat liver, adipocytes, and rat and human erythrocytes" *Tonyobyo (Tokyo, Japan)*, **1982**, *25(11)*, 1165-1170.

31. Garusinghe, G.S.P.; Bessey, S.M.; Bruce, A.E.; Bruce, M.R.M. "The influence of gold(I) on the mechanism of thiolate, disulfide exchange" *Dalton Trans*., **2016**, *45*, 11261

32. Gough, J.D.; Williams, R.H.; Donofrio, A.E.; Lees, W.J.; "Folding disulfide-containing proteins faster with an aromatic thiol" *J. Am. Chem. Soc.*, **2002**, *124*, 3885-3892

33. Ke, C.; Yin, D.; Sun, W.; Zhang, Q.; "Refolding of denatured/reduced lysozyme by aromatic thiols in the absence of small molecule disulfide" *Res. Chem. Intermed*., **2015**, *41*, 5859-5868.

34. Garusinghe, G.; Bessey, S.M.; Aghamoosa, M.; McKinnon, M.; Bruce, A.E.; Bruce, M.R.M.; "Disulfide competition for phosphine gold(I) thiolates: phosphine oxide formation vs. thiolate disulfide exchange" *Inorganics*, **2015**, *3*, 40-54

35. Lioe, H.; Duan, M.; O'Hair, R.A.J.; "Can metal ions be used as gas-phase disulfide bond cleavage reagents? A survey of coinage metal complexes of model peptides containing an intermolecular disulfide bond" *Rapid Communications in Mass Spectrometry*, **2007**, *21*, 2727-2733.

36. Lioe, H.; O'Hair, R.A.J.; "A novel salt bridge mechanism highlights the need for nonmobile proton conditions to promote disulfide bond cleavage in protonated peptides under low-energy collisional activation" *J. Am. Soc. Mass Spectrom*., **2007**, *18*, 1109-1123.

37. Lioe, H.; O'Hair, R.A.J.; "Comparison of collision-induced dissociation and electron-induced dissociation of *singly protonated* aromatic amino acids, cystine and related simple peptides using a hybrid linear ion trap-FT-ICR mass spectrometer" *Anal. Bioanal. Chem.*, **2007**, *389*, 1429-1437.

38. Abrams, M.J.; Murrer, B.A.; "Metal compounds in therapy and diagnosis" *Science*, **1993**, *261(5122)*, 725+.

39. Best, S.L.; Sadler, P.J.; "Gold drugs: mechanism of action and toxicity" *Gold Bulletin*, **1996**, *29(3)*, 87-93.

40. Edman, J.C.; Ellis, L.; Blancher, R.W.; Roth, R.A.; Rutter, W.J.; "Sequence of protein disulfide isomerase and implications of its relationship to thioredoxin" *Nature*, **1985**, *317(19)*, 267-270.

41. Seo, A.; Jackson, J.L.; Schuster, J.V.; Vardar-Ulu, D.; "Using UV-absorbance of intrinsic dithiothreitol (DTT) during RP-HPLC as a measure of experimental redox potential *in vitro*" *Anal. Bioanal. Chem.*, **2013**, *405(19)*, 6379-6384.

42. Coates, G.E.; Kowala, C.; Swan, J.M.; "Coordination compounds of group IB metals: triethylphoshphine complexes of gold(I) mercaptides" *Aust. J. Chem.*, **1966**, *19*, 539-545

43. Stocco, G.; Gattuso, F.; Isab, A.A.; Shaw, C.F.; "Synthesis and characterization of complexes of trialkyl- and triarylphosphine gold(I) with thiolated purines and pyrimidines: a class of bifunctional compounds with potential antitumor activity" *Inorganica Chemica Acta*, **1993**, *209*, 129-135.

44. Gough, J.D.; Barrett, E.J.; Silva, Y.; Lees, W.J.; "*ortho*- and *meta*- substituted aromatic thiols are efficient redox buffers that increase the folding rate of a disulfide-containing protein" *Journal of Biotechnology*, **2006**, *125*, 39-4.

AUTHOR'S BIOGRAPHY

Anna Tyrina was born in Syktyvkar, Komi Republic, Russia on February 14th, 1997. From the age of eleven she was raised in Greenwood, Maine, and graduated from Telstar High School in 2015. Anna majored in Chemistry but worked as a Maine Learning Assistant in the Physics Department for two years. She is a member of Phi Beta Kappa. Anna has received financial assistance for her thesis research from The Charlie Slavin Research Fund of the Honors College at the University of Maine. Upon graduation, Anna plans to pursue a Master of Science in Teaching degree and integrate inquiry-based differentiated instruction into the high school classroom setting, teaching physical science.